Robust Exploration and Commercial Missions to the Moon Using LANTR Propulsion and In-Situ Propellants Derived from Lunar Polar Ice (LPI) Deposits

Stanley K. Borowski[1], Stephen W. Ryan[2], Laura M. Burke[3], David R. McCurdy[4] and James E. Fittje[4]
NASA Glenn Research Center, Cleveland, OH 44135
email: Stanley.K.Borowski@nasa.gov, telephone: (216) 977-7091

Claude R. Joyner
Aerojet Rocketdyne, West Palm Beach, FL 33410

The nuclear thermal rocket (NTR) has frequently been identified as a key space asset required for the human exploration of Mars. This proven technology can also provide the affordable "access through cislunar space" necessary for commercial development and sustained human presence on the Moon. It is a demonstrated technology capable of generating both high thrust and high specific impulse (I_{sp} ~900 s) – twice that of today's best chemical rockets. Nuclear lunar transfer vehicles – consisting of a propulsion stage using three ~16.5 klb_f "Small Nuclear Rocket Engines (SNREs)", an in-line propellant tank, plus the payload – can enable a variety of reusable lunar missions. These include cargo delivery and crewed lunar landing missions. Even weeklong "tourism" missions carrying passengers into lunar orbit for a day of sightseeing and picture taking are possible. The NTR can play an important role in the next phase of lunar exploration and development by providing a robust in-space lunar transportation system (LTS) that can allow initial outposts to evolve into settlements supported by a variety of commercial activities such as in-situ propellant production used to supply strategically located propellant depots and transportation nodes. The processing of LPI deposits (estimated to be ~2 billion metric tons) for propellant production – specifically liquid oxygen (LO_2) and hydrogen (LH_2) – can significantly reduce the launch mass requirements from Earth and can enable reusable, surface-based lunar landing vehicles (LLVs) using LO_2/LH_2 chemical rocket engines. Afterwards, LO_2/LH_2 propellant depots can be established in lunar polar and equatorial orbits to supply the LTS. At this point a modified version of the conventional NTR – called the LO_2-augmented NTR, or LANTR – would be introduced into the LTS allowing bipropellant operation and leveraging the mission benefits of refueling with lunar-derived propellants (LDPs) for Earth return. The bipropellant LANTR engine utilizes the large divergent section of its nozzle as an "afterburner" into which oxygen is injected and supersonically combusted with nuclear preheated hydrogen emerging from the engine's choked sonic throat – essentially "scramjet propulsion in reverse." By varying the oxygen-to-hydrogen mixture ratio, LANTR engines can operate over a range of thrust and I_{sp} values while the reactor core power level remains relatively constant. A LANTR-based LTS offers unique mission capabilities including short transit time crewed cargo transports. Even a "commuter" shuttle service may be possible allowing "one-way" trip times to and from the Moon on the order of 36 hours or less. If only 1% of the postulated water ice trapped in deep shadowed craters at the lunar poles were available for use in lunar orbit, such a supply could support daily commuter flights to the Moon for many thousands of years! The proposed paper outlines an evolutionary mission architecture and examines a variety of mission types and transfer vehicle designs, along with the increasing demands on LDP production as mission complexity and ΔV requirements increase. A comparison of vehicle features and engine operating characteristics are also provided together with a discussion of the propellant production and mining requirements, and issues, associated with using LPI as the source material.

---

[1]Chemical & Thermal Propulsion Systems Branch, 21000 Brookpark Road, MS: 86-8, AIAA Associate Fellow
[2]Aeronautics & Ground-Based Systems Branch, 21000 Brookpark Road, MS: 162-2, Cleveland, OH 44135
[3]Mission Architecture & Analysis Branch, 21000 Brookpark Road, MS: 162-2, Cleveland, OH 44135
[4]Vantage Partners, LLC at Glenn Research Center, 3000 Aerospace Parkway, Brook Park, OH 44142

Nomenclature

°C / °K	=	temperature (in degrees Celsius / Kelvin)
EEO	=	Elliptical Earth Orbit
IMLEO	=	Initial Mass in Low Earth Orbit
klb_f	=	thrust (1000's of pounds force)
LEO	=	Low Earth Orbit (= 407 km circular / 28.5 deg inclination)
LLO	=	Low Lunar Orbit (= 300 km circular / equatorial)
LLO_2 / LLH_2	=	Lunar-derived Liquid Oxygen / Liquid Hydrogen
LPO	=	Lunar Polar Orbit (= 300 km circular)
LTV	=	Lunar Transfer Vehicle
NERVA	=	Nuclear Engine for Rocket Vehicle Applications
NLTV	=	Nuclear-powered Lunar Transfer Vehicle
O/H MR	=	Oxygen-to-Hydrogen Mixture Ratio
SLS / HLV	=	Space Launch System / Heavy Lift Vehicle
t	=	metric ton (1 t = 1000 kg)
ΔV	=	velocity change increment (km/s)

I. Introduction and Background

Today there is considerable discussion within NASA, the Congress and industry regarding the future direction and focus of the United States' human space program. According to NASA, the direction and focus is a "Journey to Mars" [1] sometime around the mid-to-late 2030's. However, while NASA's sights are set on Mars, there is another destination of interest to the worldwide space community – the Moon. Located just 3 days from Earth, the Moon is an entire world awaiting exploration, future settlement and potential commercialization. It has abundant resources and is an ideal location to test and demonstrate key technologies and systems (e.g., surface habitation, long-range pressurized rovers, surface power and resource extraction systems) that will allow people to explore, work, and live self-sufficiently on another planetary surface.

Despite NASA's past "been there, done that" attitude towards the Moon, a human lunar return mission has strong appeal to many others who would like to see humans again walk on its surface. With the upcoming 50th anniversaries of the Apollo 8 orbital mission of the Moon (on December 24-25, 1968) and the Apollo 11 landing mission (on July 20-21, 1969) fast approaching, lunar missions are again a topic of considerable discussion both within NASA [2] and outside. Plans for human surface missions and even settlements on the Moon in the 2025 – 2030 timeframe are being openly discussed by Europe, China, and Russia [3,4,5]. A number of private companies in the United States – SpaceX [6], Bigelow Aerospace (BA) [7], Shackleton Energy Company (SEC) [8], United Launch Alliance (ULA) [9], and Blue Origin [10] – are also discussing commercial ventures to the Moon, along with possible public-private partnerships with NASA.

This past February, Space X announced [6] that it would send two tourists on a week-long, "free return" flyby mission around the Moon in 2018 – undoubtedly to capitalize on the significance of NASA's historic Apollo 8 mission. In early March, Bigelow Aerospace discussed its plans [7] to launch a private space station into LEO by 2020 using ULA's Atlas V launch vehicle. The station would use the BA-330 habitat module possessing ~330 m^3 of internal volume once inflated. The company went on to say that a variant of the BA-330 module could also be placed in LLO to serve as a transportation node / refueling depot for astronauts and spacecraft making their way to and from the Moon and the lunar surface.

Lunar-derived propellant (LDP) production – specifically LLO_2 and LLH_2 – has been identified as a key technology offering significant mission leverage [11] and it figures prominently in both SEC's and ULA's plans [8,9] for commercial lunar development. Samples returned from different sites on the Moon during the Apollo missions have shown that the lunar regolith has a significant oxygen content. The iron oxide (FeO)-rich volcanic glass beads returned on the final Apollo (17) mission have turned out to be a particularly attractive source material for oxygen extraction based on hydrogen reduction experiments conducted by Allen et al. [12]. Post-Apollo lunar probe missions have also provided orbital data indicating the possible existence of large quantities of water ice trapped in deep, permanently shadowed, craters located at the Moon's poles [13]. This data has generated considerable excitement and speculation, including plans for a commercial venture by SEC [8] that proposes to mine LPI, convert it to rocket propellant, and then sell it at propellant depots located in LEO.

Besides providing an ideal location for testing surface systems and "in-situ" resource utilization (ISRU) equipment, lunar missions also provide a unique proving ground to demonstrate an important in-space technology – Nuclear Thermal Propulsion (NTP). With its high thrust and high specific impulse (I_{sp} ~ 900 s) – twice that of today's best chemical rockets – the NTR can play an important role in *"returning humans to the Moon to stay"* by enabling a reusable in-space LTS that provides the affordable access through cislunar space necessary for initial lunar outposts to evolve into thriving settlements engaged in a variety of commercial activities.

Over the past three decades, engineers at Glenn Research Center (GRC) have analyzed NTP's use for lunar missions, quantified its benefits and developed vehicle concept designs for a variety of exploration and commercial mission applications [14,15,16,17]. A sampling of these vehicle concepts and mission applications is shown in Fig. 1. Also shown is a transition away from vehicles using a single high thrust engine (Fig. 1a) to vehicles using clustered lower thrust engines (Figs.1b–1e) to help reduce development costs and increase mission safety and reliability by providing an "engine out" capability.

The NTR achieves its high specific impulse by using LH_2 to maintain the reactor fuel elements at their required operating temperature then exhausting the heated hydrogen gas exiting the reactor out the engine's nozzle to generate thrust. Because the NTR is a monopropellant engine, a key question emerges *"How can the high performance of the NTR and the leverage potential of LDP best be exploited?"* The answer is *the "LO_2-Augmented" NTR (or LANTR) – a LH_2-cooled NTR outfitted with an O_2 "afterburner nozzle" and feed system* [18,19,20]. Combining NTR and supersonic combustion ramjet engine technologies, LANTR is a versatile, high performance engine that can enable a robust nuclear LTS with unique capabilities and can take full advantage of the mission leverage provided by using LDPs by allowing "bipropellant" operation.

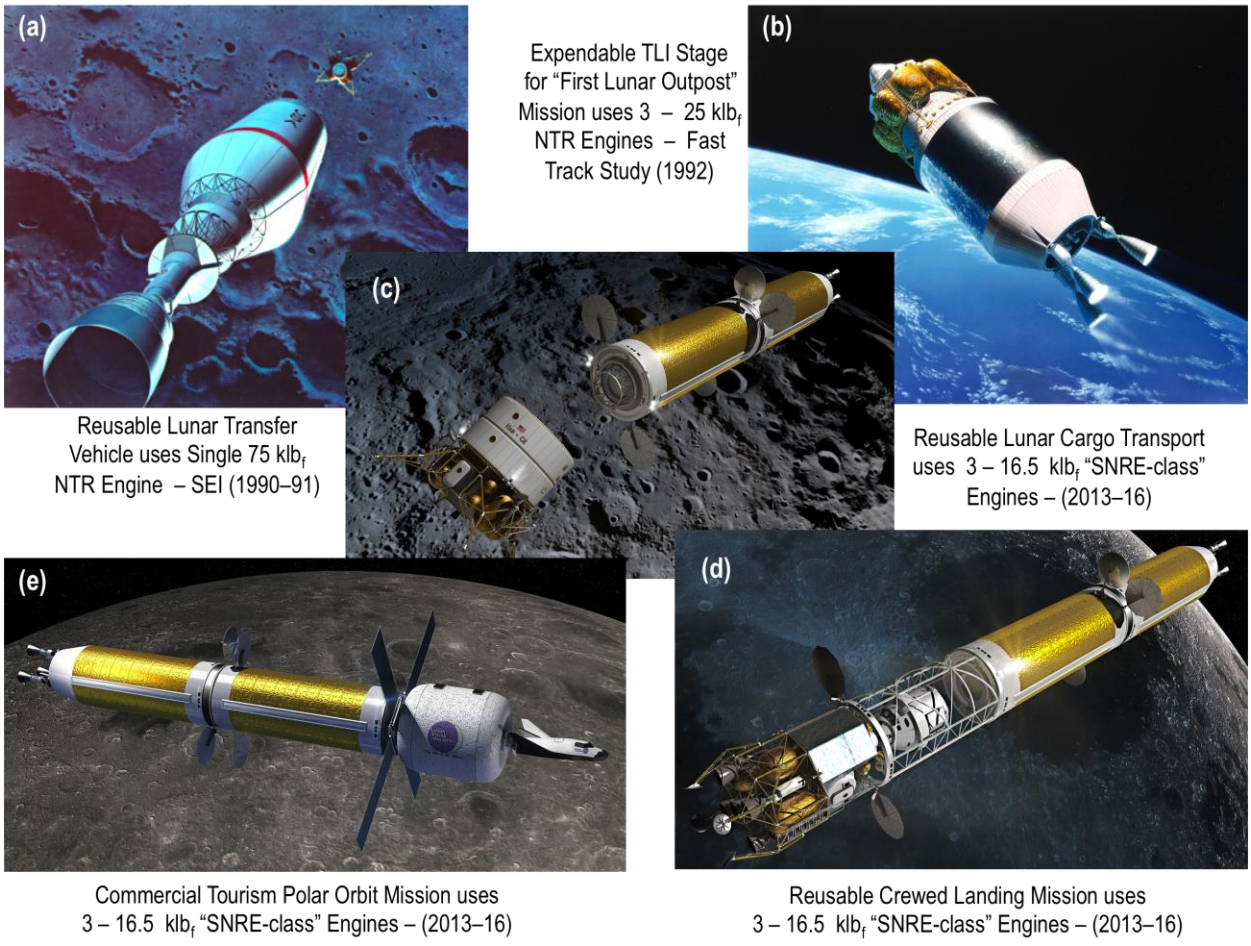

Figure 1. Sampling of Past and Recent Crewed, Cargo and Commercial Lunar Transfer Vehicles Designed by GRC Shows a Transition Away from Single Large to Multiple Smaller Engines

In light of the current interest being expressed in LDPs [8,9], GRC engineers have been re-examining the impact of infusing LANTR propulsion into a nuclear-powered LTS that utilizes LDPs. The author (Borowski) presented a paper on this topic 20 years ago at the 33rd Joint Propulsion Conference in Seattle, Washington [18]. In that work, the primary LDP and feedstock material considered was LLO_2, also referred to as LUNOX, and FeO-rich volcanic glass beads, and only Earth-supplied LH_2 (ELH_2) was used in the LANTR LTS. The decision to use LUNOX back then was based on an extensive set of hydrogen reduction experiments [21,22] that established "*ground truth*" for oxygen release from samples of lunar soil and volcanic glass beads returned by the Apollo missions. The highest yields – in the range of 4-5 weight percent (wt%) – were obtained from the iron-rich volcanic glass samples [21,22] collected during the Apollo 17 mission to Taurus-Littrow (Fig 2). Another important consideration was the identification of a significant number of large pyroclastic "dark mantle deposits" (DMDs) containing this glassy material on the lunar nearside just north of the "equatorial corridor" [23,24].

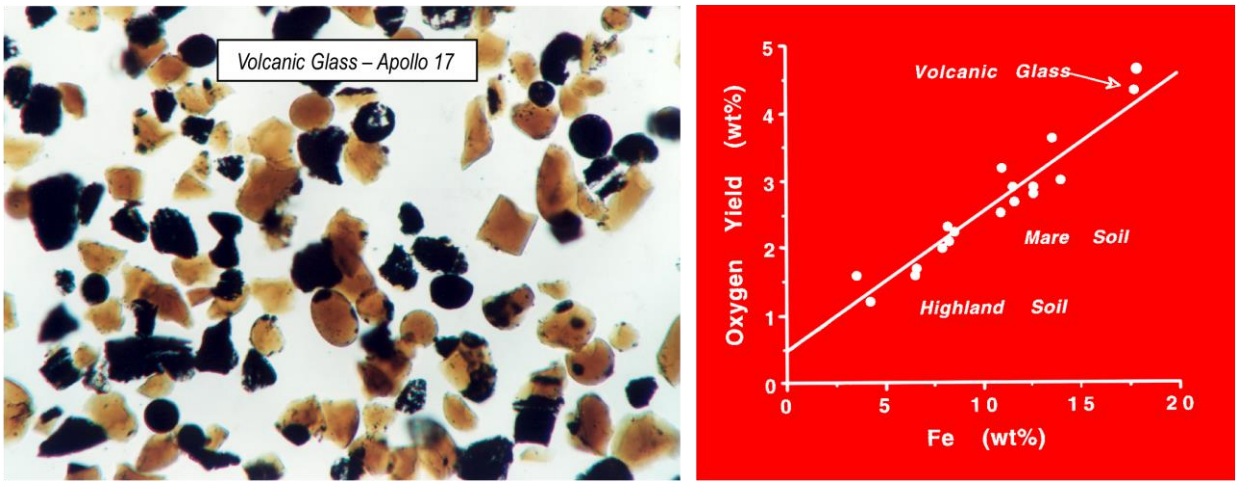

Figure 2. Volcanic Glass Beads and Oxygen Yields from Full Range of Apollo samples [22]

This same degree of certainty cannot be claimed for LPI. While considerable enthusiasm has been expressed about mining and processing LPI for rocket propellant, and using it to create a space-faring cislunar economy [25], the ground truth about LPI must first be established before this enthusiasm is warranted. Robotic surface missions will be required to quantify the physical state of the water ice, its vertical thickness and areal extent, and the levels of soil contamination. Also, the permanently shadowed craters, where LPI is thought to exist, are deep and extremely cold posing major challenges for mining and processing any cold, ice-bearing regolith that might be uncovered [26]. These conditions may negate the apparent advantage that LPI has over volcanic glass as a feedstock material – namely, the ability to provide a source of both LLH_2 as well as LLO_2.

There are also many scientifically interesting sites on the Moon that are far from the lunar poles. For example, the Aristarchus Plateau (~27°N, 52°W) is located in the midst of a vast DMD that can supply the feedstock material needed to produce LUNOX. Access to this nearside, near-equatorial site should also be relatively easy. If a decision were made to locate a research station or base there, producing oxygen locally would probably make more sense rather than incurring the added complexity and cost of transporting it from the poles. Finally, oxygen extraction from iron-rich mare soil or volcanic glass has an additional benefit – it also produces useful metals (iron and titanium) which using LPI feedstock does not.

Despite the uncertainties regarding LPI mentioned above, this paper examines the potential mission impact of using LPI-derived LLO_2 and LLH_2 together with LANTR propulsion in an evolving LTS. The paper provides a summary of our ongoing analysis results to date and includes the following topics. First, the benefits and options for using LDPs are discussed including the use of LUNOX. Then the scientific data supporting the possible existence of water ice trapped within deep, permanently shadowed craters at the Moon's poles is reviewed and proposed concepts for its mining are discussed. Next, a system description of the NTR and the LANTR concept is presented along with performance projections for the engine as a function of the oxygen-to-hydrogen mixture ratio used in the afterburner nozzle. The mission and transportation system ground rules and assumptions used in our analysis are then provided and used in an evolutionary mission architecture that illustrates the benefits of using LANTR and LDP quantifying them in terms of reduced vehicle size, launch mass and required engine burn times. The potential

for a robust, reusable LTS that includes short transit time crewed cargo transports and commuter shuttles is discussed next along with the refueling needs and production rates needed to support these more demanding and higher ΔV missions. These results are compared to similar missions, discussed in a previous paper [27], that operate out of equatorial LLO and use only LLO_2 derived from volcanic glass. The paper ends with some concluding remarks and thoughts on the possibilities for future human expansion into the Solar System using LANTR propulsion and sources of locally produced extraterrestrial propellant.

II. Benefits of Using and Options for Producing Lunar-Derived Propellants

Previous studies conducted by NASA and its contractors [28,29] have indicated a substantial benefit from using lunar-derived propellants – specifically LLO_2 in the lunar space transportation system. In a LTS using LO_2/LH_2 chemical rockets, ~6 kilograms (kg) of mass in LEO is required to place 1 kg of payload on the lunar surface (LS). Of this 6 kg, ~70% (4.2 kg) is propellant and ~85.7% of this mass (3.6 kg) is oxygen assuming the engines operate with an O/H MR of 6:1. Since the cost of placing a kilogram of mass on the LS is ~6 times the cost of delivering it to LEO [11], the ability to produce and utilize LLO_2 from processed lunar volcanic glass or regolith, or LLO_2 and LLH_2 from the electrolysis of LPI, can provide a significant mission benefit. By providing a local source of oxygen and hydrogen for use in life support systems, fuel cells and the chemical rocket engines used on LLVs, the IMLEO, launch costs and LTS size and complexity can all be reduced. Greater quantities of "higher value" cargo (e.g., people, ISRU equipment and scientific instruments) can also be transported to LEO and on to the Moon instead of bulk propellant mass further reducing LTS costs.

Pyroclastic Deposits of Volcanic Glass: The Lunar "Persian Gulf" for Future LUNOX Production?

As mentioned in the Introduction, samples brought back on the Apollo missions have shown that nearly half the mass (~43%) of the Moon's surface material is oxygen [11] and at least 20 different techniques [30,31] have been identified for its extraction. The FeO-rich volcanic glass beads returned on the final Apollo (17) mission have turned out to be a particularly attractive source material for oxygen extraction using the hydrogen reduction process. The two-step process produces iron and water that is then electrolyzed to obtain oxygen and hydrogen – a portion of which is recycled back as the catalyst – while the oxygen is liquefied and stored.

Reduction experiments conducted by Allen et al. [22,32] have shown the glassy (orange) and crystalline (black) beads to be an attractive feedstock producing oxygen yields of ~4.3 wt% and 4.7 wt%, respectively – the highest obtained from all of the Apollo samples tested. These glassy and crystalline beads are unconsolidated, fine-grained (see Fig. 2) and can be fed directly into a LLO_2 production plant with little or no processing prior to reduction.

More importantly, a significant number of large pyroclastic deposits, thought to be the result of continuous, Hawaiian-style, fire-fountain eruptions from large vents, have been identified on the lunar nearside by Gaddis et al, [24]. These deposits are of regional extent and are composed largely of crystallized black beads, orange glass beads, or a mixture of the two. Noteworthy large deposits located just north of the lunar equator include: (1) the Aristarchus Plateau (~49,015 km^2); (2) Southern Sinus Aestuum (~10,360 km^2); (3) Rima Bode (~6,620 km^2); (4) Sulpicius Gallus (~4,320 km^2); (5) Southern Mare Vaporum (~4,130 km^2); and (6) Taurus Littrow (~2,940 km^2). At the smallest of these deposits, Taurus Littrow – located at the southeastern edge of Mare Serenitatis – the largely black crystalline beads found there are thought to be tens of meters thick and could produce well in excess of a billion metric tons of LUNOX using the hydrogen reduction process, a 4.5 wt% oxygen yield and a 5 m mining depth.

LPI: Its Possible Location and Estimated Quantities

Watson et al. first conjectured about the existence of water ice at the lunar poles in 1961 [33]. Later in 1979, Arnold [34] estimated the mass of water deposited in permanently shadowed craters at the lunar poles over the last 2 billion years at ~10 - 100 billion metric tons and concluded that the lunar poles might provide an abundant water resource for future exploitation. The sources for this water were attributed to micrometeoroids, solar wind proton reduction of lunar regolith, and comets.

Recently, the *Clementine* [35], *Lunar Prospector* [36], *Chandrayaan-1* [37] *Lunar Reconnaissance Orbiter* (*LRO*) [38] and *Lunar CRater Observation and Sensing Satellite* (*LCROSS*) [39] lunar probe/impact missions have provided data indicating the possible existence of large quantities of water ice (estimated at 100's of millions to billions of metric tons) trapped within a number of deep, perpetually dark craters found near the Moon's poles.

The first spacecraft to observe the lunar poles in detail was *Clementine*, a joint Department of Defense and NASA probe launched in 1994. Using an onboard transmitter, *Clementine* beamed radio waves into the dark regions of the Moon's south polar region including the Shackleton crater (Fig. 3). Echoes of these waves were subsequently detected back on Earth using the large dish antennas of the Deep Space Network. The polarization characteristics of the echoes from this "bistatic radar experiment" [35] were interpreted as evidence of possible water ice.

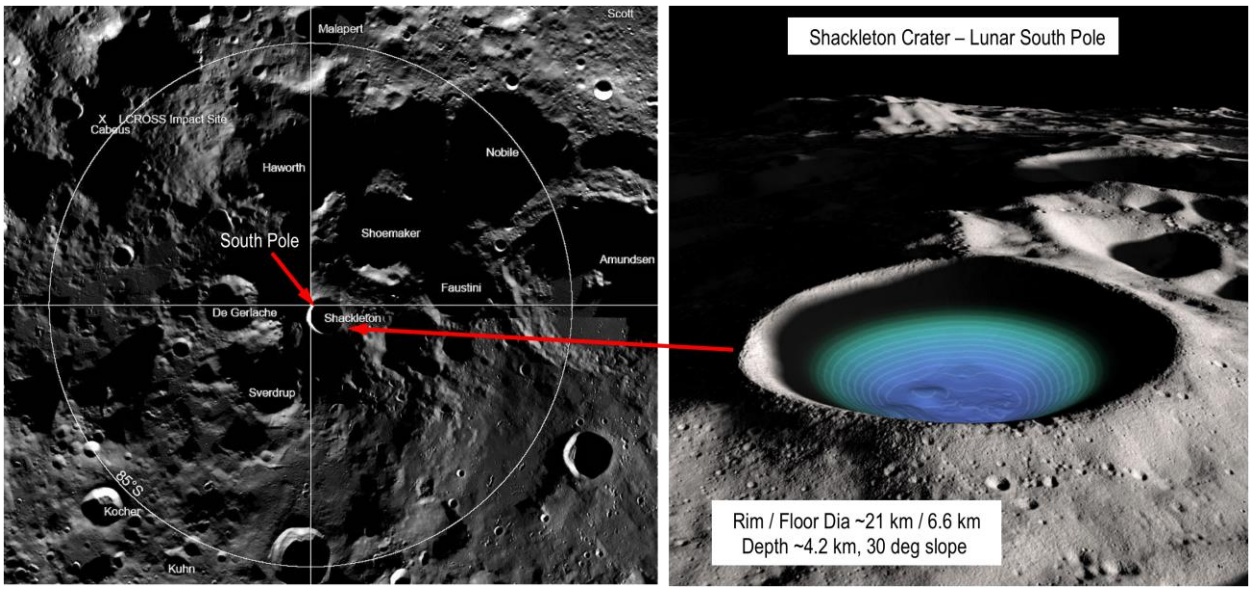

Figure 3. Lunar South Polar Region and Features of Nearby Shackleton Crater

Four years later, in 1998, the *Lunar Prospector* probe was launched. It carried a neutron spectrometer to measure the amount of hydrogen in the lunar regolith near the polar regions. The *Lunar Prospector* science team found enhanced hydrogen concentrations at the north and south poles that were interpreted as indications of significant amounts of water ice (~1.5 +/- 0.8 wt% in the regolith) contained within a number of these polar "cold traps". Based on estimates of the shadowed crater areas, the total quantities of water ice were estimated by Feldman et al. [36] to be ~135 - 240 million metric tons in the south polar region and ~62 million metric tons in the north. If all of the enhanced hydrogen inventory measured by *Lunar Prospector's* neutron spectrometer was in the form of water ice crystals, Feldman et al. estimated the total amount of water at both poles to be ~2 billion metric tons.

In October 2008, India's first lunar probe, *Chandrayaan-1*, was launched carrying with it NASA's Mini-SAR (Synthetic Aperture Radar). From February to April 2009, Mini-SAR mapped more than 95% of the Moon's polar regions extending from 80° latitude to the poles [40]. On March 1, 2010, NASA announced that the Mini-SAR had discovered more than 40 permanently shadowed, super-cold craters located within 10° of the Moon's north pole (shown in Fig. 4). The craters ranged in size from 2 to 15 km in diameter and the amount of water ice they might contain was estimated to be ~600 million metric tons [37].

The search for LPI continued with NASA's *LRO* / *LCROSS* mission launched in June 2009. Onboard *LRO* was a Miniature Radio Frequency (Mini-RF) instrument specifically designed to map the Moon's polar regions, including the permanently shadowed "cold trap" areas, and analyze the scattering properties of the RF signal in an effort to characterize the physical nature of the deposits that exist there [38]. A key parameter obtained from this scattered RF signal is the circular polarization ratio (CPR). High values of CPR can indicate the presence of water ice but they can also be attributed to the surface roughness of a crater. Using *LRO's* Mini-RF imaging radar system, Spudis et al. [38] identified a large number of "anomalous" polar craters that exhibited high CPR values only in their interiors, interiors that are permanently dark and very cold (< 100 °K). According to Spudis, these anomalously high CPR deposits exhibit behavior consistent with the presence water ice. If this interpretation is correct, Spudis estimated that several hundred million metric tons of relatively "clean" water ice may exist in the upper 2-3 m of the lunar surface at both poles [38].

Additional data on the existence and quantity of polar ice was obtained by *LRO's* companion satellite, *LCROSS*. On October 9, 2009, the *Centaur* upper stage of the *Atlas V* launch vehicle was directed to impact with the south

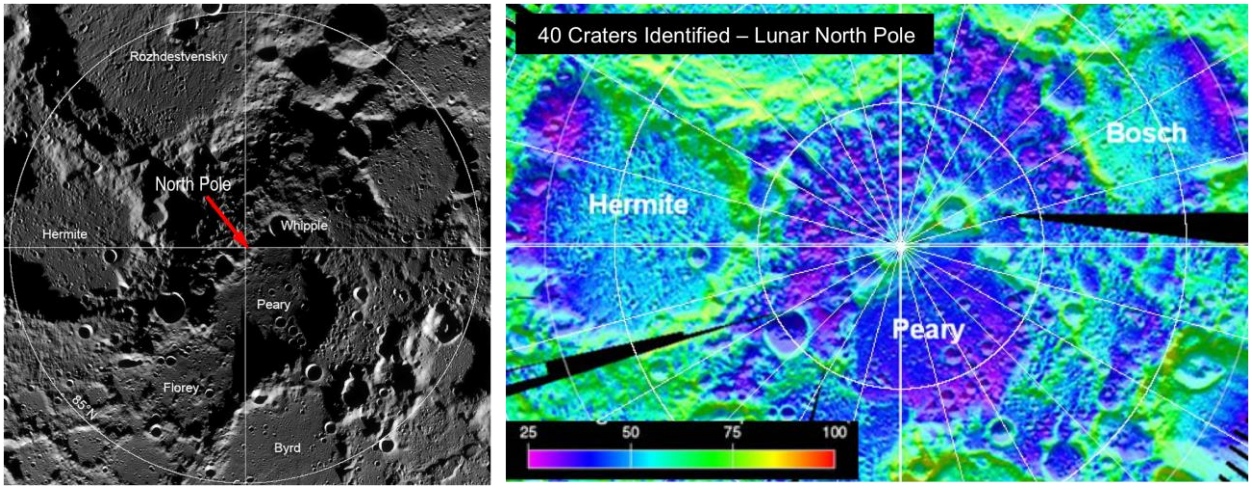

Figure 4. Lunar North Polar Region and Measured Temperatures in Nearby Craters

polar crater, Cabeus, shown in the upper left corner of Fig. 3. Shortly after impact, the *LCROSS* spacecraft flew through the ejecta plume and attempted to detect the presence of water vapor in the debris cloud. Analysis of spectrometry data indicated the spectral signature of water and a later definitive analysis by Colaprete et al. [39] determined the concentration of water ice in the regolith at the impact site to be ~5.6 +/- 2.9 wt%. On the basis of the data provided from the above lunar probe missions, it therefore appears that the concentration of water ice in the polar regolith can vary anywhere from ~1-10 wt% and total quantities of LPI at both poles can range from ~600 million to ~2 billion metric tons.

Environmental Conditions and Proposed Concepts for Mining Lunar Polar Ice

Lunar polar ice deposits are a potential important resource because the recovered water can be electrolyzed to supply both oxygen and hydrogen (at a ratio of 8:1), assuming the deposits can be economically accessed, mined, processed and stored for their desired use. Higher ΔV budgets are required to access lunar polar orbit sites and the candidate craters are deep (Fig. 3), extremely cold (Fig. 4), and exist in a state of perpetual darkness, posing major challenges for mining and processing these cold ice-bearing materials.

To put the operating temperature conditions into perspective, the world's 10 coldest mines are located in Russia and all but one of these are located in Russia's Sakha Republic - a region in the country's extreme north containing vast diamond, coal and gold resources [41]. At the coldest of these mines, Sarylakh, the temperatures can drop to nearly -50 °C (~223 °K). By contrast, the temperatures inside the polar craters, where LPI is thought to exist, are ~30-50 °K – more than 5x colder than the coldest mines on Earth! In fact, the coldest temperature in the solar system measured by a spacecraft was on the floor of the crater, Hermite, located near the Moon's north pole [42]. In 2009, using its Diviner temperature instrument, *LRO* recorded a temperature of ~26 °K (-247 °C) along the southwestern edge of Hermite. Extremely cold temperatures similar to those found in Hermite were also found in the nearby craters Peary and Bosch (shown in Fig. 4) as well as at the bottoms of several permanently shadowed craters located in the Moon's south polar region. All are candidates for LPI deposits and potential mining.

In addition to working in dark, extremely cold surroundings, where metals can become brittle, mining equipment must also be designed to operate in a hard vacuum, on electricity rather than petrol, and in gravity that is 1/6th that of Earth. It must also be able to tolerate an increased radiation environment and the abrasive nature of the lunar dust that can cause increased rubbing friction, wreak havoc on machinery, and has a tendency to adhere to everything it touches [43]. On Earth, surface mining is the most common approach to mineral extraction and a variety of systems developed for terrestrial application have also been examined for mining lunar regolith [44, 45]. The mining process itself involves the following operations: fragmentation, excavation, loading, hauling and resource separation.

Mechanical mining methods frequently combine multiple operations into a single machine. For example, a mechanical excavator can be designed to break up, or fragment, the ice-bearing regolith, excavate it, and then transport it to the water extraction plant. A notional design for such a combined excavator-hauler is shown in Fig. 5. A bucket wheel excavator and conveyor digs and lifts the ice-bearing regolith to an upper dump bed until it is filled.

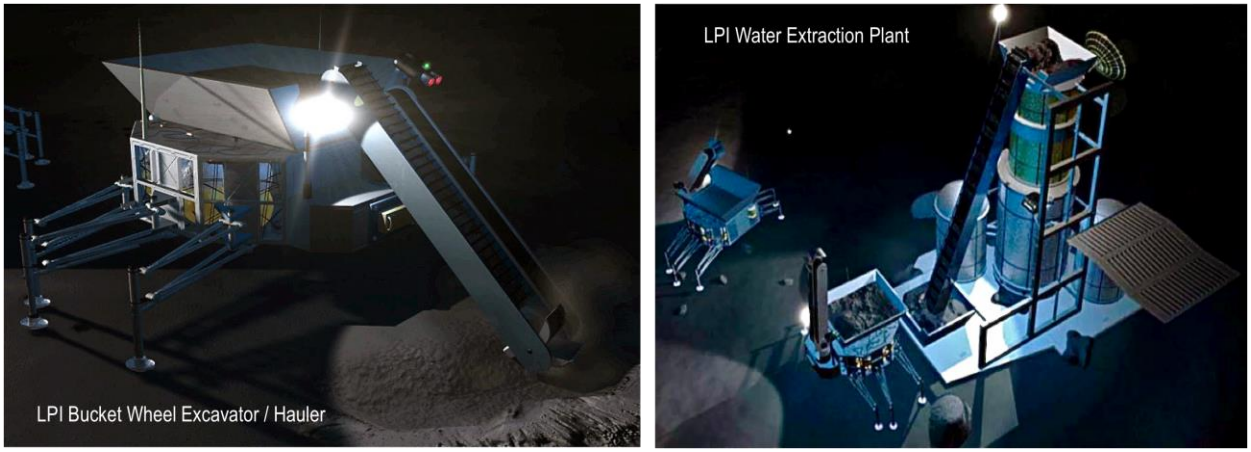

Figure 5. Notional Combination Excavator / Hauler Transports Ice-rich Regolith to Processing Plant for Water Extraction and Subsequent Propellant Production

Articulated legs on the excavator-hauler then allow it to walk over to the water extraction plant where the regolith is deposited. While one excavator-hauler empties its load, another returns to the mining site to begin the cycle again. Multiple units are used consistent with the desired production rate and the designed capabilities of the individual units. While legged vehicles have certain advantages operating on rocky ground, wheeled vehicles are more versatile and can provide faster movements on relatively smooth terrain. Wheeled vehicles are also more adaptable to teleoperations and automation then legged vehicles that have more complex movements.

During the early 1990's under NASA sponsorship, the Department of Interior's Bureau of Mines conducted a lunar surface mining equipment study and proposed two pieces of mining equipment potentially compatible with previously established design criteria, basic mining principles, and the lunar environment [45, 46]. The Ripper-Excavator-Loader (REL) and its companion Hauling Vehicle (HV), shown in Fig. 6, were conceptualized to be a multipurpose, production-class mining equipment, and were designed for teleoperation. The REL was equipped with a ripper on its back end that would be used to loosen compacted or ice-cemented regolith while its front bucket scoop would be used to excavate, self-load, and transport regolith. The HV had a rear-dump bed and was optimized for regolith hauling and higher ground speeds. Introduced as production rates increase, the HV would transport feedstock material from the mine to the processing plant and tailings from the plant back to the planned dump site.

Both vehicles used cleated, conical wheels to provide an efficient traction interface with the lunar soil, and to avoid the problems of abrasive wear that tracked vehicles would encounter with their many moving parts. Each wheel was driven by a separate electric motor and a hydrogen/oxygen fuel cell system provided power to each vehicle. The onboard hydrogen and oxygen tanks would be refilled and the leftover water reprocessed at an electrolysis station powered by a surface nuclear power plant.

Figure 6. Combination REL and Supporting HV for Production-class LPI Mining Operations

Although lacking specific quantitative details, Gustafson and Rice [47] outlined three basic approaches for extracting lunar ice. The first involves in-situ heating of the ice/regolith mixture without excavation using a mobile rover with a microwave generator aimed at the soil. As the regolith is heated from within, and ice turns to vapor and is collected on cold plates located within a domed cover placed over the area being processed. The solid ice would then be removed from the cold plates and transported out of the shadowed crater in storage tanks mounted on a fuel cell-powered rover. While a number of design issues must be considered (e.g., the choice of frequency, the dielectric properties of the regolith, and the electrical-to-microwave energy conversion efficiency), the microwave extraction process [48] is envisioned to be simpler, less disruptive, and more "environmentally friendly" to the surrounding lunar surface.

In the second approach, the ice/regolith mixture is mechanically excavated and processed within the cold trap using a water extraction furnace that uses nuclear or solar energy as the heat source. The liquid or gaseous water is then transported to a collection site outside of the shadowed crater for filtration, purification and storage. The third option excavates the fragmented ice-rich regolith using a dragline bucket [44] that transports it from the cold trap to a sunlit area outside the crater for processing. Each of these concepts has its advantages and disadvantages.

Before detailed mining and water extraction systems can be designed and evaluated, the material characteristics of the ice/regolith (e.g., its physical properties, the form, concentration, and spatial resolution of ice within the regolith) needs to be determined. NASA's *Resource Prospector* (RP) mission [49], with a planned 2021 launch date, will use onboard neutron and infrared spectrometers and a drill (capable of obtaining samples from a depth of ~1 m), to: (1) characterize the nature and distribution of water and other volatiles in lunar polar subsurface material; (2) demonstrate the extraction and capture of native water; and (3) demonstrate the extraction of oxygen from the lunar regolith using the hydrogen reduction process.

In the meantime, tests are being conducted and measurements made using simulated ice/regolith mixtures in laboratory settings here at Earth. Gertsch et al. [50, 51] have analyzed the effects of varying water ice content (from 0 to ~12 wt%) in a lunar regolith simulant (JSC-1) to determine the effect on the excavatability of different ice-regolith mixtures. Load-penetration tests were conducted on compacted samples cooled to 77 K (using LN_2) to simulate conditions expected in lunar cold traps. Based on the measured values of specific penetration (used to predict material excavatability and uniaxial compressive strength) and specific energy (used to predict excavator power and production rate), Gertsch et al. matched the different ice-regolith mixtures to the following types of terrestrial mined rocks: (1) at 0 to ~0.3 wt% ice – mixture behaves like weak coal that is easy to excavate; (2) at ~0.6 to 1.5 wt% ice (similar to that measure by *Lunar Prospector*) – mixture behaves like weak shale or mudstone and is readily excavatable; (3) at ~8.4 wt% ice (similar to that measure by *LCROSS*) – mixture behaves like moderate strength limestone, sandstone and is excavated using mechanical excavators; and (4) at ~10 to 12 wt% ice – mixture behaves like strong limestone, sandstone, and high strength concrete that requires massive excavators. According to Gertsch, a dual-focused program of material characterization and excavator design and testing will be required [50] to develop a robust rotating cutterhead [51] with the capabilities needed to mine lunar ice deposits in the future.

III. NTR / LANTR System Description and Performance Characteristics

The NTR uses a compact fission reactor core containing "enriched" uranium (U)-235 fuel to generate 100's of megawatts of thermal power (MW_t) required to heat the LH_2 propellant to high exhaust temperatures for rocket thrust [52]. In an "expander cycle" engine (shown in Fig. 7), high pressure LH_2 flowing from a turbopump assembly (TPA) is split into two paths with the first cooling the engine's nozzle, pressure vessel, neutron reflector, and control drums, and the second path cooling the engine's core support tie-tube assemblies. The flows are then merged and the heated H_2 gas is used to drive the TPAs. The hydrogen turbine exhaust is then routed back into the reactor pressure vessel and through the internal radiation shield and upper core support plate before entering the coolant channels in the reactor's fuel elements. Here it absorbs energy produced from the fission of U-235 atoms, is superheated to high exhaust temperatures (T_{ex} ~2700 °K or more depending on the uranium fuel loading), then expanded out a high area ratio nozzle (~300:1) for thrust generation.

Controlling the NTR during its various operational phases (startup, full thrust and shutdown) is accomplished by matching the TPA-supplied LH_2 flow to the reactor power level. Multiple control drums, located in the reflector region surrounding the reactor core, regulate the neutron population and reactor power level over the NTR's operational lifetime. The internal neutron and gamma radiation shield, located within the engine's pressure vessel, contains its own interior coolant channels. It is placed between the reactor core and key engine components to prevent excessive radiation heating and material damage.

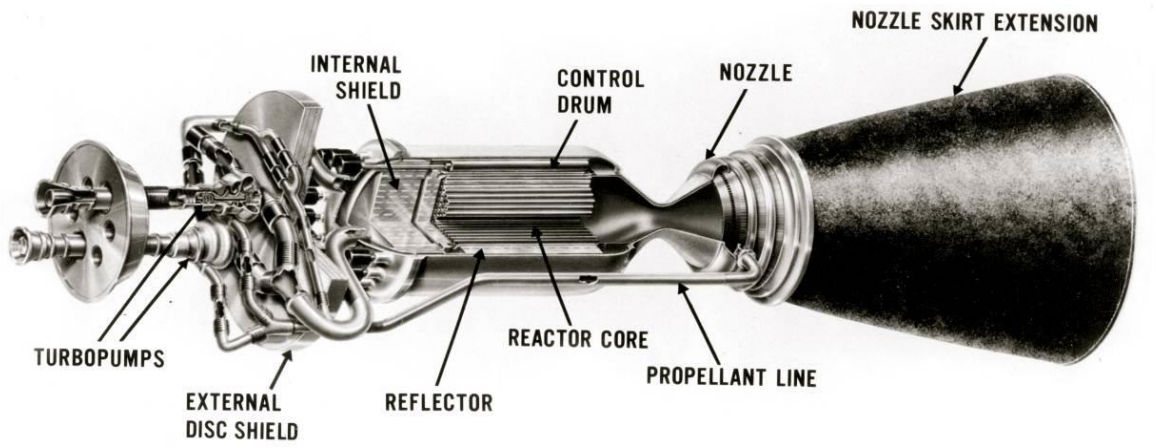

Figure 7. Schematic of "Expander Cycle" NTR Engine with Dual LH_2 Turbopumps

Recent studies showing the benefits of NTP for a variety of exploration and commercial lunar missions [16,17] have used a "common" Nuclear Thermal Propulsion Stage (NTPS) employing a cluster of three SNREs. The engine's reactor core is composed of hexagonal-shaped fuel elements and core support tie tubes developed and tested during the Rover/NERVA program [52]. Each fuel element (FE) was fabricated using a "graphite matrix" material that contained the U-235 fuel in the form of either coated particles of uranium carbide (UC_2) or as a dispersion of uranium and zirconium carbide (UC-ZrC) referred to as "graphite composite" (GC) fuel (see Fig. 8).

This higher performance GC fuel was developed as a *"drop-in replacement"* for the coated particle fuel and was tested in the Nuclear Furnace element test reactor (NF-1) [52] near the end of the Rover program. The GC elements achieved a peak power density of ~5 MW_t per liter (~5000 MW_t/m^3) and a peak fuel temperature of ~2700 °K. The GC elements also demonstrated better corrosion resistance than the standard coated particle fuel elements used in the previous Rover/NERVA reactor tests. This improved resistance of the GC fuel was attributed to its higher coefficient of thermal expansion (CTE) that more closely matched that of the protective ZrC coating, thereby helping to reduce coating cracking. Electrical-heated composite fuel elements were also tested by Westinghouse in hot hydrogen at 2700 K for ~600 minutes – equivalent to ten 1-hour cycles.

Heritage Rover/NERVA FEs had a hexagonal cross section (~0.75 inch across the flats) and 19 axial coolant channels (shown in Fig. 10) that were coated with niobium carbide (NbC) initially, then with zirconium carbide (ZrC) using a chemical vapor deposition (CVD) process. This protective coating, applied to the FE's exterior surfaces as well, helped to reduce coating cracking, hydrogen penetration and subsequent erosion of the graphite matrix material. Individual elements were 1.32 m (52 inches) in length and produced ~1 MW_t during steady state, full power operation. Also included in the engine's reactor core were hexagonal-shaped tie tube (TT) elements that provided structural support for 6 surrounding FEs (shown in Fig. 8). A coaxial Inconel tube inside the TT carries hydrogen coolant that is then used to supply a source of heated hydrogen for turbine drive power in the SNRE's expander cycle engine design. A sleeve of zirconium hydride (ZrH) moderator material is also incorporated into each TT (see Fig. 8) to help increase core reactivity and allow construction of smaller, lower thrust engine systems like the Small Nuclear Rocket Engine (SNRE) [52] developed by Los Alamos National Laboratory near the end of the Rover/NERVA program.

Although it was not built, the SNRE incorporated all of the lessons learned from the program's 20 previous reactor designs and test results. The FE had the same hexagonal cross section and coolant channel number, but was 35 inches long, used GC fuel, and produced ~0.65 MW_t. To help increase core reactivity, the "SNRE" FE – TT pattern increased the number of TTs so that each FE has 3 adjacent TTs and 3 adjacent FEs surrounding it (Fig. 8). With the SNRE pattern, the FE to TT ratio is ~2 to 1 with each tie tube providing redundant mechanical support for six surrounding fuel elements.

The baseline SNRE used in this study has a nominal power output of ~365 MW_t, an average power density of ~3.44 MW_t/liter, and produces ~16.5 klb_f of thrust. The reactor core has 564 fuel elements and 241 tie tubes, and is surrounded by a 14.7 cm thick perimeter neutron reflector resulting in a pressure vessel diameter of ~98.5 cm. With a fuel loading of ~0.6 g/cm^3, the SNRE's FEs contain ~60 kg of 93% enriched U-235. The GC fuel operates at a

peak temperature of ~2860 °K and the corresponding hydrogen exhaust temperature is ~2734 °K. With a chamber pressure of 1000 psia, a hydrogen flow rate of ~8.30 kg/s and a nozzle area ratio (NAR) of ~300:1, the engine's I_{sp} is ~900 s. The total engine length is ~5.8 m with the ~1.8 m long radiation-cooled, retractable nozzle section fully extended. The nozzle exit diameter is ~1.53 m and the engine's thrust-to-weight ratio is ~3.02.

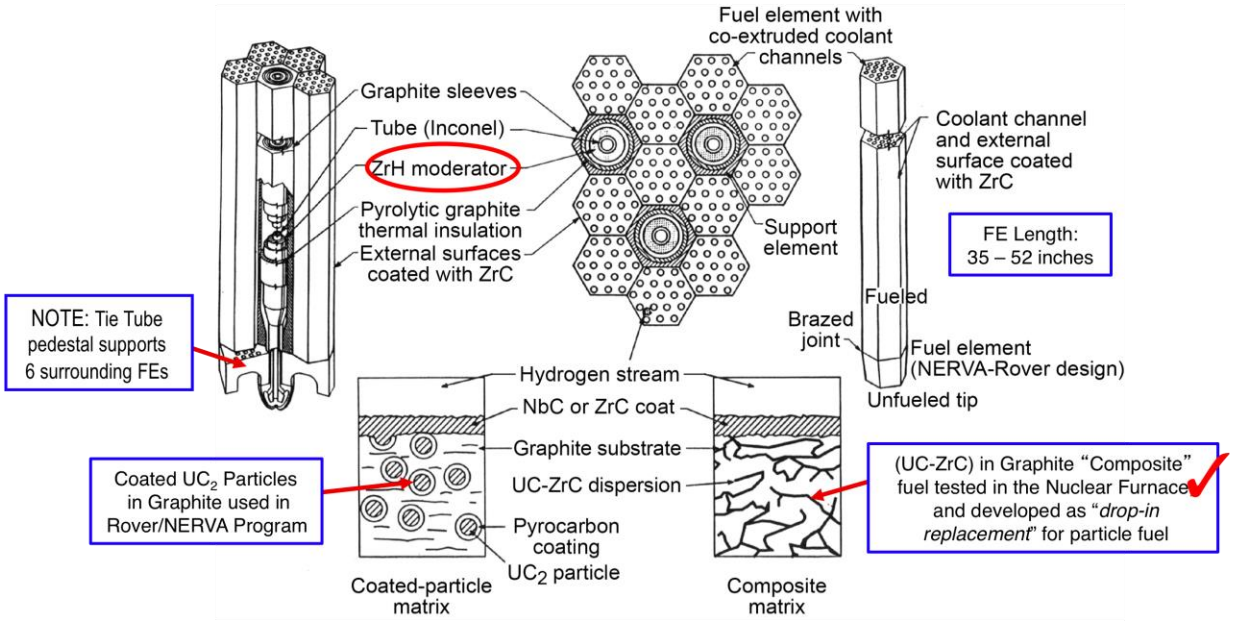

Figure 8. Coated Particle and Graphite Composite SNRE Fuel Element and Tie Tube Arrangement

LANTR: An Enhanced NTR with "Bipropellant" Operational Capability

In order to take full advantage of LLO_2 once it becomes available to the LTS, each SNRE is outfitted with an O_2 "afterburner" nozzle containing the O_2 injectors and an O_2 feed system. The oxygen is stored as a cryogenic liquid at low pressure and must be pressurized and gasified prior to its injection into the nozzle. This is accomplished by diverting a small fraction of the engine's hydrogen flow (~3%) to an oxidizer-rich gas generator that drives a LO_2 TPA used to deliver the gasified LO_2 to injectors positioned inside the afterburner nozzle downstream of the throat [18,19,20]. Here it mixes with the hot H_2 and undergoes supersonic combustion adding both mass and chemical energy to the rocket exhaust – essentially *"scramjet propulsion in reverse."*

Downstream nozzle injection in LANTR isolates the reactor core from oxygen's damaging effects provided the throat retains choked flow. This operating condition can be satisfied by using a "cascade" scramjet injector developed by Aerojet [20] – now Aerojet Rocketdyne. A 3-zone staged injection approach [20] is envisioned using multiple cascade injectors to control the oxygen addition and heat release within the nozzle while keeping the flow supersonic. This approach also increases penetration, mixing and combustion of the injected oxygen within the hydrogen flow while minimizing shock losses and the formation of high heat flux regions, thereby maximizing engine performance and life. A high reactor outlet pressure is also desirable since it allows the use of a high area ratio nozzle – important for increasing combustion efficiency – at reasonable size and mass.

A simplified schematic of LANTR engine operation is illustrated in Fig. 9. Also shown is a photograph of a non-nuclear, "proof-of-concept" demonstration test of a LANTR nozzle that used a "fuel-rich" 2100 lb_f chemical rocket engine operating at a oxygen/hydrogen MR <2 to simulate a NTR. The water-cooled, copper test nozzle had NAR of 25:1 and used 3 wedge-shaped injectors (2 of which are visible in Fig. 9) [53]. These tests and follow-on tests with a 50:1 nozzle indicated that up to 73% of the injected oxygen burned within these short nozzles resulting in an augmented thrust level of ~53% as measured on the engine thrust stand [20].

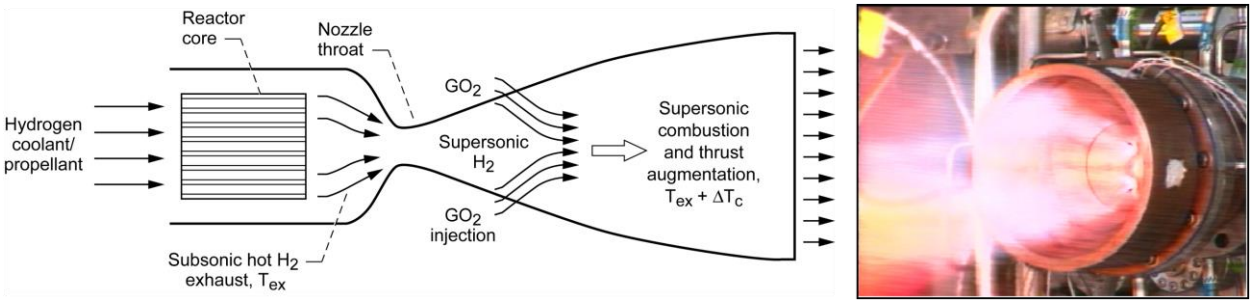

Figure 9. Simplified LANTR Schematic and Simulated "Proof-of-Concept" Test Article Photograph [53]

The LANTR concept has the potential to be an extremely versatile propulsion system. By varying the O/H MR, the LANTR engine can operate over a wide range of thrust and I_{sp} values – shown in Table 1 – while the reactor core produces a relatively constant power output. As the MR varies from 0 to 5, the engine thrust level for the SNRE increases by over 344% – from 16.5 klb_f to ~56.8 klb_f – while the I_{sp} decreases by ~57% – from 900 to 516 s which is still 54 s higher than that achieved by today's best LO_2/LH_2 chemical engine – the RL10B-2 [54]. This thrust augmentation feature means that "big engine" performance can be obtained using smaller, more affordable LH_2-cooled NTR engines that are easier to build and less costly to test on the ground. The engines can then be operated in space in the augmented high thrust mode to shorten burn times (thereby extending engine life) and reduce gravity losses (thereby eliminating the need for and concern over using a multiple "perigee burn" Earth departure maneuver). Lastly, the increased use of high-density LO_2 in place of low-density LH_2, and the ability to resupply or "reoxidize" LANTR vehicles with LLO_2 prior to Earth return, are expected to significantly reduce vehicle size and mass while increasing delivered payload.

Table 1. SNRE / LANTR Performance Characteristics as a Function of O/H Mixture Ratio

O/H Mixture Ratio	0	1	2	3	4	5
Delivered I_{sp} (s)	900**	725	637	588	552	516
Thrust Augmentation Factor	1.0	1.611	2.123	2.616	3.066	3.441
Thrust (lb_f)	16,500	26,587	35,026	43,165	50,587	56,779
Engine Mass (lb_m)	5,462	5,677	5,834	5,987	6,139	6,295
Engine T/W	3.02	4.68	6.00	7.21	8.24	9.02

** Fuel Exit / Hydrogen Exhaust Temperature = 2734 °K , Chamber Pressure = 1000 psia and NAR = 300 to 1

IV. Mission, Payload and Transportation System Ground Rules and Assumptions

Specific mission and payload ground rules and assumptions used in this paper are summarized in Table 2. It provides information about the different lunar mission scenarios, along with the assumed parking orbits at Earth and the Moon. Specific trajectory details and ΔV budgets for the different missions examined are provided within the appropriate sections of the paper. In addition to the large ΔV requirements for the primary propulsion maneuvers, like trans-lunar injection (TLI), smaller ΔV maneuvers are needed for propellant settling, vehicle mid-course correction (MCC) maneuvers, orbital operations in LPO, including rendezvous and docking (R&D) of the LTV with surface-based LLVs or with the lunar propellant depot, and lastly LTV-depot separation and station keeping.

A variety of different payloads are also considered. On initial "all LH_2" NTR crewed landing missions, a forward mounted saddle truss is used to connect the payload elements to the transfer vehicle's in-line tank. The truss is open on its underside and its forward adaptor ring provides a docking interface between the MPCV and the single stage

Table 2. Mission and Payload Ground Rules and Assumptions

• Crewed lunar landing using NTR (3 day transits to and from the Moon with 3 – 14 days on the surface) • Crewed cargo transport using LANTR (1.5 – 3 day transits to and from the Moon with 3 days in LPO) • LANTR commuter shuttle carries Passenger Transport Module (PTM) ("1-way" transit of 36 hours or less)	• Reusable LTV carries MPCV, reusable LLV and surface payload to LPO; returns MPCV and spent LLV to EEO; Orion capsule used for crew recovery at mission end • Reusable, LANTR LTV transports habitat module, crew, and varying amounts of cargo, depending on the transit times to and from LPO; LTV refuels with LDP at a LPO depot before returning to Earth • Reusable, LANTR LTV transports a PTM to LPO for subsequent delivery to the lunar surface by LLV; LTV refuels with LDP at a LPO depot before returning to Earth with another PTM
• NTR / LANTR missions depart from LEO and capture / depart from LPO; NTR missions return to EEO while LANTR missions return to LEO	• LEO: 407 km circular • LPO: 300 km circular • 2.86-hr EEO: 407 km x 7,316 km • 24-hr EEO: 500 km x 71,136 km
• Primary mission ΔV maneuvers: NTR or LANTR engines used • Additional ΔV requirements: Advanced Material Bipropellant Rocket (AMBR) RCS thrusters used to perform non-primary propulsion maneuvers as well as primary burn maneuvers under 100 m/s	• ΔV budgets for different missions discussed in appropriate sections • Propellant settling burn: ~1 m/s • Mid-course correction: ~10 m/s • Lunar orbit R&D & maintenance: ~40 m/s • Depot separation & station keeping: ~10 m/s
• Crewed landing mission payload masses: Reusable NTR LTV delivers *Orion* / MPCV and single stage LO_2 / LH_2 Lunar Descent / Ascent Vehicle (LDAV) to LLO; LDAV carries 4 crew and 5 t of payload to lunar surface; LTV with *Orion* / MPCV, LDAV and surface samples returned to a 24-hr EEO	• *Orion* / MPCV: 13.5 t • Saddle truss assembly (STA) 7.2 t • LDAV crew cab & dry mass: 8.6 t • Crew (4) & EVA suits: 0.8 t • LDAV propellant load: 20.9 – 22.4 t • LDAV surface payload: 5.0 t • Returned Samples: 0.1 t
• Crewed cargo transport payload masses: Reusable LANTR LTV delivers a habitat module, crew and cargo (10 – 20 t depending on the transit time) from LEO to LPO then returns to LEO	• Habitat Module: 9.9 t • Single Star Truss w/RMS: 5.29 t • Outbound Payload: 4-8 cargo pallets (2.5 t each) • Crew (4) & EVA suits: 0.80 t • Returned Samples: 0.25 t
• Commuter shuttle payload mass: Reusable LANTR LTV delivers a PTM from LEO to LPO then back again	• PTM: 15 t (includes 2 crew & 18 passengers)

LO_2/LH_2 LDAV (shown in Fig. 10a). The LDAV is a "heritage" design [55] analyzed in considerable detail during NASA's earlier Space Exploration Initiative (SEI) studies. It carries a crew of 4 plus 5 t of surface payload (PL) stored in two 2.5 t PL pallets mounted on each side of the crew cab. The LDAV mass breakdown including the propellant loading and landed payload is shown in Table 2. On the lunar landing mission analyzed here, the crew collects and returns ~100 kg of samples.

Delivered to LPO by a NTR-powered cargo transport, a 36 t "wet" LLV – without a crewed PL and ascent stage – is capable of delivering ~28 t to the lunar surface. Assuming it can be configured to fit within the SLS-1B PL shroud, the landed PL can take the form of a fully functional habitat lander, a processing plant for LPI, or various pieces of heavy mining equipment such as the notional rotating bucket-wheel excavator shown in Fig. 10b. Without any attached PL, the NTR cargo transport can also function as a propellant "tanker" delivering over 27 t of Earth-supplied LH_2 to a LPO depot on each roundtrip mission.

For the reusable, space-based crewed cargo transport missions using LANTR propulsion and LDP on the Earth return mission leg, the LTV carries a habitat module that supports a crew of 4. Two crewmembers operate the vehicle and manage the unloading of the PL. The other 2 represent rotating crewmembers on assignment at the lunar base or the LPO transportation node / propellant depot. Connecting the habitat module to the rest of the LANTR LTV is a "star truss" that has four concave sides to accommodate four PL pallets (shown in Fig. 10c). The forward circular truss ring also has a Remote Manipulator System (RMS) with twin arms attached to it. Using the habitat module's rear viewing window, the crew uses these arms to unload and attach the transport's cargo to the depot node or to a co-orbiting LLV transferring crew and awaiting cargo delivery.

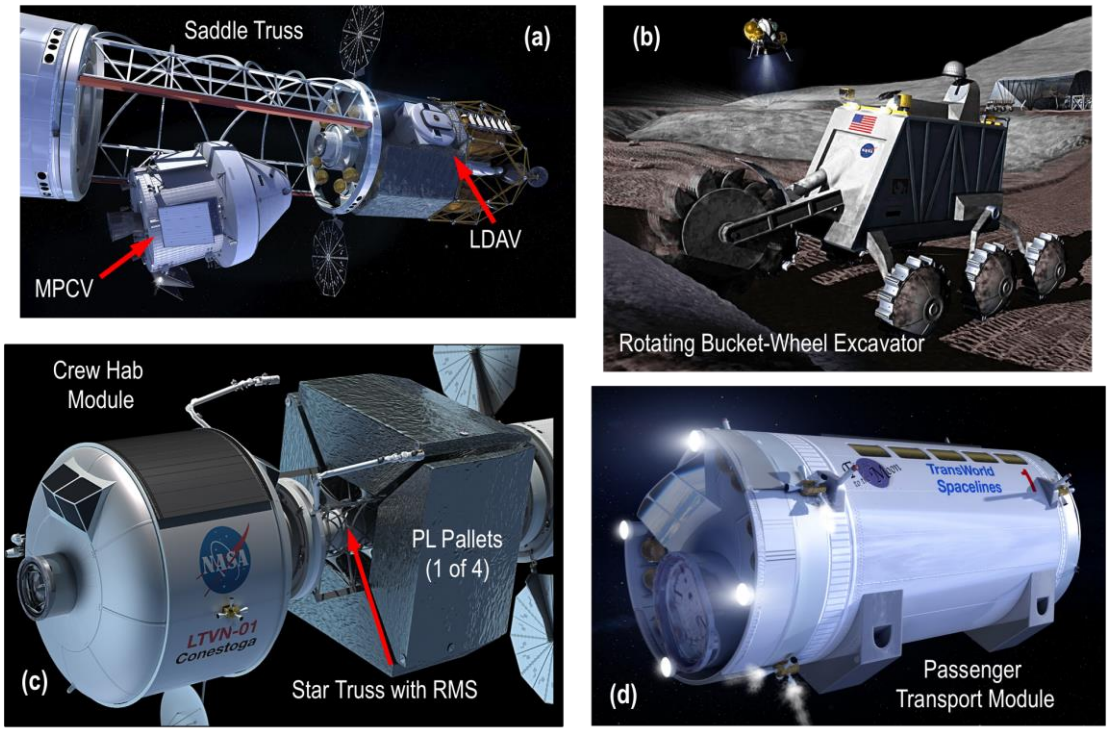

Figure 10. Payload Elements Carried by the NTR and LANTR Lunar Transfer Vehicles

Using the same LANTR LTV system elements shown in Fig. 11, routine commuter flights to and from the Moon can also be considered. For the commuter shuttle application, the cargo transport's habitat module, star truss and PL pallets are removed and replaced with a PTM (Fig. 10d) that carries 18 passengers and 2 crew members.

Table 3 lists the key ground rules and assumptions used in the NTR / LANTR transportation system elements. The NTPS carries only LH_2 and uses three clustered SNRE-class engines initially before transitioning over to LANTR operation. The smaller diameter in-line LO_2 tank located forward of the NTPS carries only LO_2. It is assumed the LANTR LTVs operating out of LPO refuel with LLO_2 primarily but are also able to "top off" their NTPS for Earth return using the excess LLH_2 produced at the LPO depot during the H_2O electrolysis process. Details on the NTR and LANTR engine design and performance are provided in Sect. II and summarized in Table 3. The total mission LH_2 and LO_2 propellant loadings consist of the usable propellant plus performance reserve and tank-trapped residuals. Additional LH_2 is also provided for engine cooldown after each major propulsive maneuver.

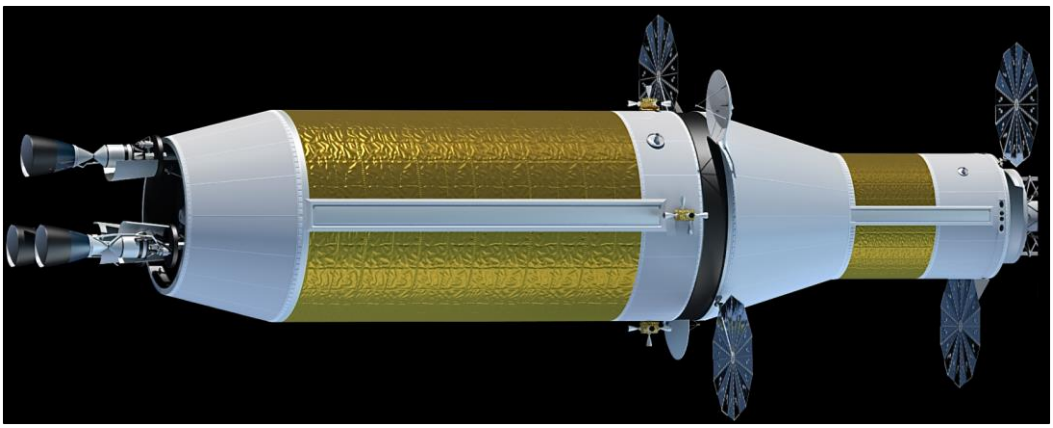

Figure 11. Key LANTR LTV System Elements – the LH_2 NTPS and In-Line LO_2 Tank

Table 3. NTR and LANTR Transportation System Ground Rules and Assumptions

NTR / LANTR Characteristics	• Engine / Fuel Type: NERVA-derived / UC-ZrC "Composite" • Propellants: LH_2 (NTR), LH_2 and LO_2 (LANTR) • Thrust Level: 16.5 klb_f SNRE-class engine using LH_2 only 26.5 klb_f – 56.8 klb_f with LANTR (MR = 1 to 5) • Fuel Element Length: 0.89 m (SNRE baseline) • Exhaust Temp: T_{ex} ~2734 °K (with 2860 °K peak temperature) • Chamber Pressure: p_{ch} ~1000 psi • Nozzle Area Ratio: ε~300:1 • I_{sp} Range: 900 s – 516 s with LANTR (MR = 0 to 5)
Propellant Margins	• Cooldown: 3% of usable LH_2 propellant • Performance reserve: 1% on ΔV • Tank trapped residuals: 2% of total tank capacity
Reaction Control System (used for Propellant Settling, MCC, Lunar Orbit Operations, and primary maneuvers under ~100 m/s)	• Propulsion Type: AMBR 200 lb_f thrusters • Propellant: NTO / N_2H_2 • Nominal I_{sp}: 335 seconds
LH_2 Cryogenic Tanks and Passive Thermal Protection System (TPS)	• Material: Aluminum-Lithium (Al/Li) • Tank OD: 7.6 m (LH_2); 7.6 m and 4.6 m (LO_2) • Tank L: 15.65 m ("core" NTPS and "in-line" LH_2 tanks) 5.23 m – 7.95 m ("in-line" LO_2 tank) • Geometry: cylindrical with root 2/2 ellipsoidal domes • Insulation: 1" SOFI (~0.78 kg/m^2) + 60 layers of MLI (~0.90 kg/m^2)
Active Cryo-Fluid Management / Zero Boil-Off (ZBO) LH_2 Propellant System	• Reverse turbo-Brayton ZBO cryocooler system powered by PVAs • ZBO system mass and power requirements driven by core stage size; ~760 kg and ~5.26 kW_e (7.6 m D)
Photovoltaic Array (PVA) Primary Power System	• Circular PVA sized for ~7 kW_e at 1 A.U, two arrays provide power for ZBO cryocoolers on core stage, PVA mass is ~566 kg for two ~25 m^2 arrays, second array set provides power to mission payloads • "Keep-alive" power supplied by lithium-ion battery system
Dry Weight Contingency Factors	• 30% on NTR system & composite structures (e.g., saddle and star trusses) • 15% on established propulsion, propellant tanks, spacecraft systems
SLS / SLS Upgrade Launch Requirements: – Usable Payload Delivered to LEO – Cylindrical Payload (PL) Envelope	• ~70 t to LEO (407 km circular) • 7.6 m OD x ~26.5 m L

For the smaller auxiliary and primary propulsion maneuvers under ~100 m/s, a storable bipropellant Reaction Control System (RCS) with AMBR thrusters is used (details in Table 3). The LANTR LTV utilizes a split RCS with approximately half the AMBR thrusters and bipropellant mass located on the rear NTPS and the other half located at the front end of the in-line LO_2 tank just behind the mission-specific payload.

The LH_2 propellant carried in the NTPS is stored in the same "state-of-the-art" Al/Li LH_2 propellant tank being developed for the SLS/HLV to support future human exploration missions. Sizing of the LH_2 tank assumes a 30 psi ullage pressure, 5 g_E axial / 2.5 g_E lateral launch loads, and a safety factor of 1.5. A 3% ullage factor is also assumed. The in-line LO_2 tank with its rear conical adaptor section uses the same sizing and launch load assumptions. All tanks use a combination spray-on foam (SOFI) / multilayer insulation (MLI) system for passive thermal protection. A zero boil-off (ZBO) "reverse turbo-Brayton" cryocooler system is used on the NTPS to eliminate LH_2 boil-off from the NTPS during the course of the mission. A passive thermal protection system is used on the in-line LO_2 tank since it is drained after the lunar orbit capture (LOC) burn and is subsequently refueled with LLO_2 before the trip back to LEO. The heat load on the NTPS hydrogen tank is largest in LEO and sizes the ZBO cryocooler system. Two sets of circular solar photovoltaic arrays (PVAs) – each producing ~14 kW_e – are baselined with one set supplying the primary electrical power needed for all key LTV sub-systems and the second set providing power for the different mission payloads considered here.

Table 3 also provides the assumed "dry weight contingency" (DWC) factors, along with the requirements for delivered mass to LEO and the shroud cylindrical payload envelope for the upgraded SLS / HLV. A 30% DWC is used on the NTR and LANTR systems and advanced composite structures (e.g., stage adaptors, trusses) and 15% on heritage systems (e.g., Al/Li tanks, RCS, etc.). The NTPS mass (~70 t) and size (~7.6 m OD and ~26.5 m length) determines the required lift capability and the usable shroud PL volume for the upgraded SLS. The combined saddle truss (~13.7 m) and LDAV (~9.6 m) used on the crewed landing mission (shown below in Fig. 12b) has this same approximate length. On the crewed cargo transport mission discussed in Sect. VII, the habitat module (~6.5 m OD and ~8.5 m in length) and star truss (~11 m in length) can be launched together, or the truss can be launched together with the in-line LO_2 tank and its conical adaptor (~11.5 m in length).

V. Performance Impact of Integrating LANTR and LDP into the LTS Architecture

As mentioned in the Introduction, the author presented a paper on the enhanced mission capability resulting from the combined use of LANTR propulsion and LUNOX 20 years ago at the 33rd Joint Propulsion Conference in Seattle, Washington [18]. In that paper, an evolutionary LTS architecture was analyzed that began with a LTS using high performance NTP to maximize delivered surface payload on each mission. The increased PL was dedicated to installing modular LUNOX production units with the intent of using this LDP to supply surfaced-based LLVs initially, then in-space LTVs using LANTR propulsion, at the earliest possible opportunity. This section re-examines this evolutionary LTS architecture to see how recent NLTV designs and missions [16,17] are impacted by the introduction of LANTR and the ability to refuel with LLO_2 and LLH_2 from a propellant depot located in LPO.

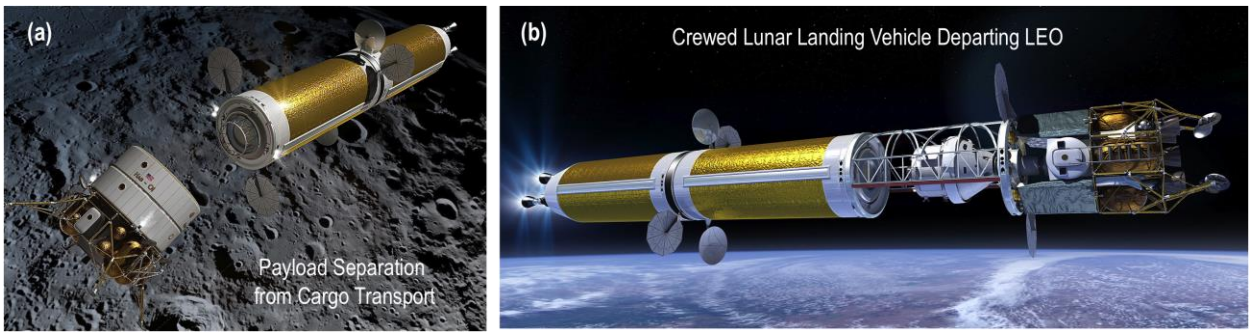

Figure 12. Reusable NTR Cargo Delivery and Crewed Lunar Landing Vehicles

The NTPS, with its three 16.5 klb_f SNREs, is the "workhorse" element on the cargo and crewed NLTVs shown in Figs. 12a and 12b. It has a 7.6 m diameter by ~15.7 m long Al/Li tank that carries ~39.8 t of LH_2 propellant. Housed within and mounted on the forward cylindrical adaptor section of the NTPS are the RCS, avionics, batteries, two deployable circular PVAs, a docking system, along with a reverse turbo-Brayton cryocooler system for zero boil-off LH_2 storage. The cryocooler system mass and power requirements increase with tank diameter and are sized to remove ~42 watts of heat penetrating the 60 layer MLI system while the stage is in LEO where the highest tank heat flux occurs. To remove this heat load, the 2-stage cryocooler system requires ~5.3 kW_e for operation

The second major element is an "in-line" Al/Li LH_2 tank that connects the NTPS to the forward PL element. It has the same diameter but a longer length (~17.1 m) than that used in the NTPS and supplies an additional ~43.9 t of LH_2 propellant used during for the "single burn" TLI maneuver. The in-line tank element also includes forward and aft cylindrical adaptor sections that house quick connect/disconnect propellant feed lines, electrical connections, a RCS along with docking and payload adaptors. A ZBO cryocooler system is not used on the in-line LH_2 tank since it is drained during the TLI maneuver. The total length of the in-line element is ~22.1 m.

Reusable Lunar Cargo Delivery / Propellant Tanker Missions

Using the NTPS and in-line tank discussed above, the NTR cargo transport can deliver ~63.6 t of cargo to LPO then return to Earth for refueling and reuse. Three SLS-1B launches deliver the vehicle and payload elements to LEO where assembly occurs via autonomous R&D. The cargo transport then departs from LEO (ΔV_{TLI} ~3.414 km/s including g-losses of ~302 m/s) and arrives at the Moon ~72 hours later. It then begins a 3-burn LOC maneuver that

places it into a 300-km circular LPO (ΔV_{LOC} ~888 m/s with g-losses). The first LOC burn captures the cargo transport into a highly elliptical orbit around the Moon with a perigee altitude of 300 km – the same as the final parking orbit. The second burn is performed at apogee to change the plane of the orbit to match the inclination of the desired parking orbit – in this case 90° for LPO. The third and final burn is performed near perigee to lower the orbit's apogee resulting in the final 300-km circular LPO. *The duration of the LOC maneuver can range anywhere from an additional several hours to as much as a day with the shorter durations requiring a larger ΔV_{LOC}.*

Once in orbit, the PL with its LLV separates from the cargo transport (shown in Fig. 12a) and descends to the surface, landing autonomously at a predetermined location near one of the lunar poles. As mentioned in the previous section, the usable PL that can be delivered by LLV is on the order of ~28 t and, assuming it can be configured to fit within the SLS-1B PL shroud, can take the form of a fully functional habitat lander, a processing plant for LPI, or various pieces of heavy mining equipment. Without any attached PL, the NTR cargo transport can also function as a propellant "tanker" delivering over 27 t of Earth-supplied LH_2 to a LPO depot on each roundtrip mission.

After payload separation and a day or so in LPO, the cargo transport performs the trans-Earth injection (TEI) maneuver (total ΔV_{TEI} ~865 m/s including g-losses) then returns to Earth 72 hours later. Like the capture burn, the TEI maneuver uses three burns as well. The first burn raises the apogee of the orbit, resulting in a highly elliptical orbit around the Moon. The second burn is a plane change burn performed near apogee that adjusts and aligns the plane of the elliptical orbit from 90° to that needed for departure. The third and final burn is again performed near perigee and after it's completed, the NLTV has escaped the Moon and is on a 3-day trajectory back to Earth.

On final approach, the cargo transport performs a braking burn (ΔV_{EOC} ~356 m/s) and captures into a 24-hour EEO with a 500-km perigee x 71,136-km apogee. Post burn engine cool-down thrust is then used to assist in orbit lowering. Afterwards, an auxiliary tanker vehicle, operating from a LEO servicing node/propellant depot, rendezvouses and docks with the cargo vehicle and supplies it with the additional LH_2 propellant needed for final orbit lowering and rendezvous with the LEO transportation node where it is refurbished and resupplied before its next mission.

The cargo NLTV has an IMLEO of ~192 t consisting of the NTPS (~68.8 t), the in-line tank element (~56.9 t), plus the PL element (~63.6 t) with its connecting structure (2.7 t). The mission requires six primary burns by the SNRE engines that use ~74.8 t of LH_2 propellant – the two small plane change burns under 40 and 20 m/s are performed using the RCS. With ~49.5 klb_f of total thrust and I_{sp} ~900 s, the total engine burn time is ~53.2 minutes. For the propellant tanker mission, the IMLEO is ~126.5 t and the total engine burn time is ~35.4 minutes.

Reusable Crewed Lunar Landing Mission

On the crewed landing mission, the NLTV carries a forward mounted saddle truss that connects the payload elements to the transfer vehicle's in-line tank. The truss is open on its underside and its forward adaptor ring provides a docking interface between the *Orion* MPCV and the single stage LOX/LH_2 LDAV as shown in Fig. 12b. The LDAV carries a crew of 4 plus 5 t of surface payload stored in two "swing-down" pallets mounted on each side of the crew cab (shown in Fig. 13b).

Three SLS-1B launches are used to deliver the two NTR vehicle elements and the payload element to LEO for assembly via autonomous R&D. The payload element consists of the integrating saddle truss assembly (STA) plus the LDAV with its surface cargo containers. In addition to a front and rear docking capability, the STA's forward adaptor ring also carries twin PVAs and a RCS. Once assembled, the *Orion* MPCV and crew are launched and rendezvous with the NLTV positioning itself inside the STA and docking with the LDAV using the docking port and transfer tunnel mounted to the STA's forward adaptor ring (shown in Fig. 10a).

After the single TLI burn (ΔV_{TLI} ~3.389 km/s including a g-loss of ~302 m/s), the crew begins its 3-day coast to the Moon. Because the crewed NLTV carries a significant amount of payload mass (the STA, MPCV, and "spent" LDAV) back from the Moon, it uses an ~17.1 m long in-line tank to supply the required amount of LH_2 propellant needed for this reusable mission. After its 72-hour transit, the NLTV begins the LOC maneuvers (ΔV_{LOC} ~849 m/s including g-loss) required to insert itself and its payload into LPO. Like the cargo transport, the crewed NLTV uses the same 3-burn orbital insertion sequence described above.

Once in LPO, the crew enters the LDAV and separates from the transfer vehicle. After separation, the LDAV's two payload pallets are rotated 180 degrees and lowered into their landing position in preparation for descent to the lunar surface (Fig. 13b). The ΔV budget used in the Martin Marietta LDAV design [55] is ΔV_{des} ~2.115 km/s and ΔV_{asc} ~1.985 km/s. The LDAV uses five RL10A-4 engines operating with a I_{sp}~450 s and ~13.5 t of LO_2/LH_2 propellant is expended during the descent to the surface.

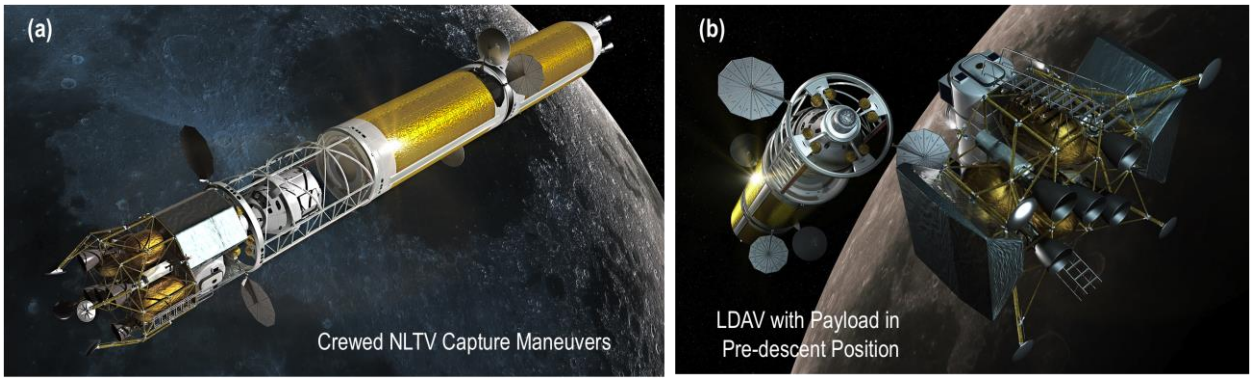

Figure 13. Crewed Lunar Landing Mission: Transfer Vehicle Capture into LPO and LDAV Landing Preparation

After completing the surface mission, the crew returns to LPO in the LDAV carrying 100 kg of lunar samples. At liftoff, the LDAV mass is ~15.1 t and ~5.5 t of propellant is used during the ascent to LPO. The LDAV then rendezvous with the transfer vehicle and preparations for the TEI maneuver begin. After completing the 3-burn departure sequence (total ΔV_{TEI} ~847 m/s with g-loss), the crew spends the next 3 days in transit readying their vehicle for the final phase of the mission – capture into a 24-hr EEO (ΔV_{EOC} ~356 m/s). Afterwards, the crew re-enters and lands using the *Orion* capsule.

The crewed lunar landing mission has an IMLEO of ~182.4 t that includes the NTPS (~69.1 t), the in-line tank assembly (~57.1 t), the STA (~7.3 t), the wet LDAV (~29.5 t) with its surface payload (~5 t), the *Orion* MPCV (~13.5 t), consumables (~0.1 t), and 4 crewmembers (~0.8 t includes lunar EVA suits). At departure, the LH_2 propellant loading in the NTPS and the in-line tank are at their maximum capacity of ~39.8 t and ~43.9 t, respectively. The overall length of the crewed NLTV is ~75.4 m. Like the cargo mission, the crewed landing mission requires 6 primary burns by the NTPS using ~79.6 t of LH_2 propellant, and the total engine burn time is again ~53.2 minutes.

Impact of Using LDP to Refuel Surface-based LDAVs and In-Space NLTVs

Figure 14 shows the variation in NLTV size, IMLEO, increased mission capability and engine burn time resulting from the development and utilization of LPI-derived LLO_2 and LLH_2. Figure 14a shows the reusable, crewed NLTV discussed above. It departs from LEO and captures into a 300-km equatorial LPO. At the end of the mission, the NLTV returns to Earth with the spent LLV and captures into a 24-hr EEO because it has a much lower ΔV requirement. In order to return to LEO, the NLTV would need an additional ~118 t of LH_2 propellant requiring the insertion of a star truss with four attached drop tanks between the vehicle's in-line tank and forward payload. The additional mass of the extra truss, propellant and tanks increases the vehicle's IMLEO to over 350 t!

The first significant step in LDP production occurs when polar outpost assets and production levels of LLO_2 and LLH_2 become sufficient to support a lunar surface-based LDAV. By not having to transport a "wet" LDAV to LPO on each flight, the crewed NLTV now has a lower starting mass in LEO (~152.2 t) plus sufficient onboard propellant to return to a lower, higher energy ~2.86-hr EEO (407 km perigee x 7,316 km apogee with ΔV_{EOC} ~1895 m/s including g-losses) as shown in Figure 14b.

After entering orbit, a surface-based LDAV, operated autonomously from the LS during liftoff, R&Ds with the crewed NLTV to pick up the crew and cargo. The cargo, consisting of two 2.5 t PL pallets, is positioned at the front end of the saddle truss ring so that the pallets readily attach on both sides of the crew cab and can subsequently be lowered into the "saddlebag" position for descent as shown in Fig. 13b. At liftoff the LDAV carries up to 22.4 t of LLO_2/LLH_2 propellant. It uses ~13 t to achieve LPO and another 9 t returning to the LS after picking up the crew and cargo. Operating at an O/H MR of ~6, the LDAV's chemical rocket engines use ~3.2 t of LLH_2 and ~19.2 t of LLO_2 propellant during its roundtrip mission to LPO and back. Because of this O/H MR and the 8:1 stoichiometry of H_2O, it will be necessary to extract and electrolyze ~28.8 t of water and overproduce on LLO_2 by ~6.4 t to obtain the required amount of LLH_2 needed to support LDAV operation between the LS and LPO and back again.

As LPI mining and LDP production levels increase further, we assume a propellant depot is established in LPO and is routinely supplied with water transported from the LS by specialized tanker LLVs. At the depot, the water is electrolyzed and the LDPs are stored for subsequent use. Periodically, the depot could also receive additional ELH_2 delivered by a NTR tanker vehicle operating between LEO and LPO. At this point, the NLTV's SNREs are refitted with afterburner nozzles and LO_2 feed systems, and the large in-line LH_2 tank used in the two previous vehicles is replaced by a smaller LO_2 tank (shown in Figure 14c). The LO_2 tank, consisting of two $\sqrt{2}/2$ ellipsoidal domes, is ~5.37 m long and has a 7.6 m diameter that is compatible with the saddle truss diameter.

In the analysis results presented in this paper, it is assumed that the LANTR LTVs operating out of LPO refuel with LLO_2 primarily but are also able to top off their NTP stages for Earth return using the excess LLH_2 produced from the H_2O electrolysis process. By refueling with ~51.4 t of LLO_2 and ~6.42 t of LLH_2 (at a ratio of 8:1), a smaller, more capable crewed NLTV Is possible. It is ~20 t lighter than the vehicle shown in Fig. 14b and can now return back to LEO as well – a significant advance in performance capability. Equally as important, the augmented thrust levels achieved during the mission decrease the total engine burn time – in this case cutting it by ~44.5%.

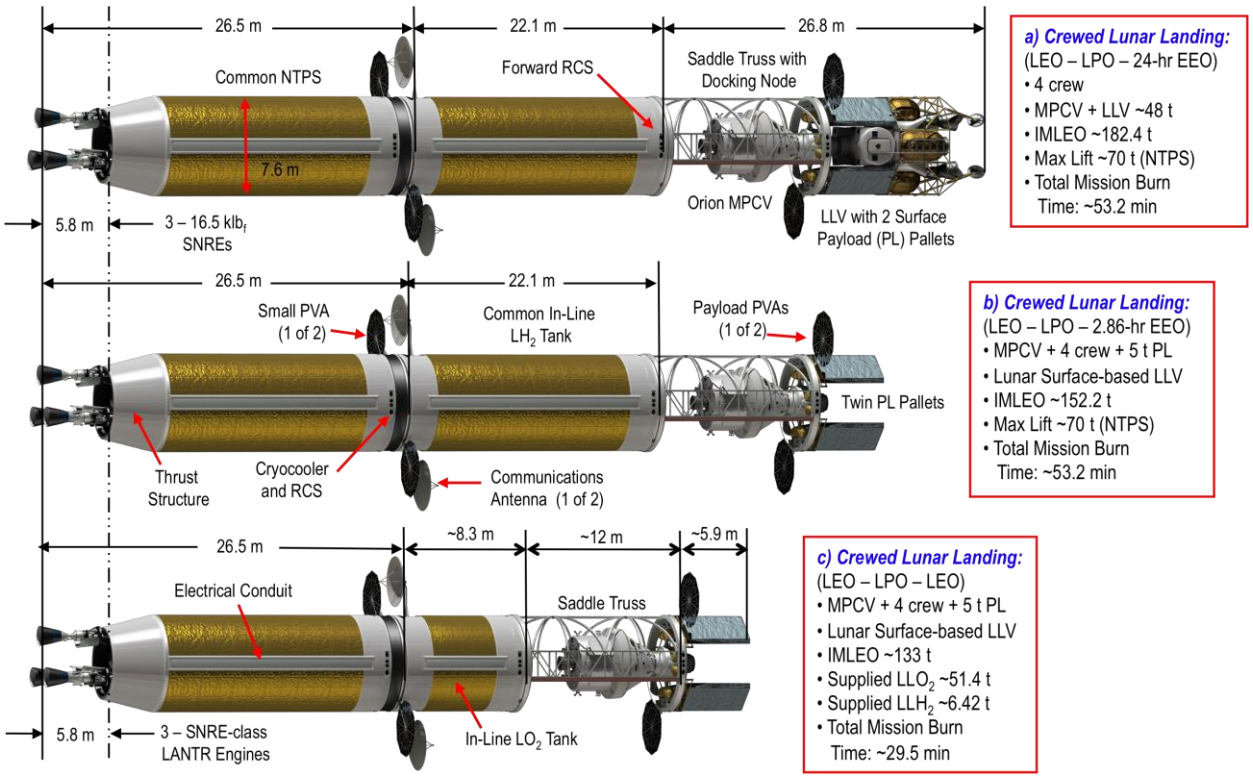

Figure 14. Variation in NLTV Size, IMLEO, Mission Capability and Engine Burn Time Resulting from the Development and Utilization of LDP and the Transition to LANTR Operation

The LANTR engines used in this study are sized with the appropriate hardware mass (pumps, controls, lines, etc) for the maximum MR operation to allow the full range of O/H MRs from 0 to 5 to be accessible during the mission. A mission analysis and vehicle sizing code with optimization capability [56] is also used to determine the propellant requirements for the various missions examined. By giving the optimizer control over the O/H MRs used for the individual mission burns as well as the initial propellant load and refueling amounts, we can find the minimum propellant requirements needed to complete the mission. Depending on the specified mission objective, the optimizer can be used to minimize the total propellant, Earth-supplied propellant, or lunar-supplied propellant usage. Alternatively, we can explore other possibilities by giving the optimizer control over cargo mass or transit times. Using this capability, we are able to determine the maximum cargo that can be delivered for a given mission scenario and vehicle configuration, along with the propellant and refueling requirements. Access to both LPI-derived LO_2 and LH_2 in LPO opens up the mission trade space and the addition of LLH_2 can be leveraged to further reduce total propellant requirements, increase payload or reduce transit times as we will discuss later in the paper.

VI. Growth Mission Possibilities Using Depots and LDP Refueling

Over time we envision the development of a totally space-based LTS with different types of NLTVs operating between transportation nodes / propellant depots located in LEO (Fig. 15a), LLO (Fig. 15b) and LPO. Because abundant deposits of volcanic glass are located at a number of sites just north of the lunar equator, a depot established in equatorial LLO would also be a good idea. These depots would be routinely supplied with LUNOX or H_2O by tanker LLVs operating between the lunar surface and either LLO or LPO. Transportation nodes/depots at these different locations would also provide convenient staging locations where crewed cargo transports can drop off PL and NTR tankers can deliver ELH_2 that would be picked up by LLVs for transport to the lunar surface.

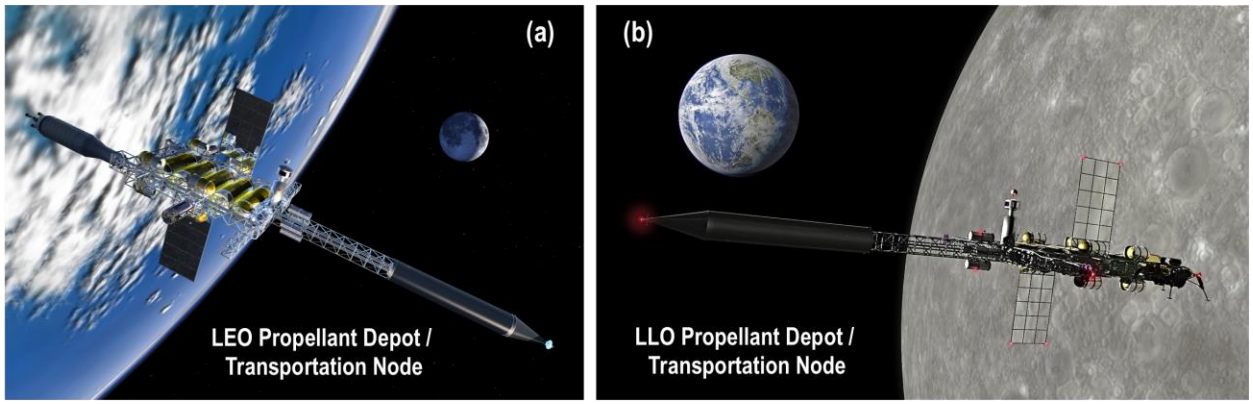

Figure 15. Propellant Depots in LEO, LLO and LPO – Critical Elements for a Robust Lunar Transportation System

One-way transit times to and from the Moon on the order of ~72 hours would be the norm initially. Eventually, however, as lunar outposts grow into permanent settlements staffed by visiting scientists, engineers and administrative personnel representing both government and private ventures, more frequent flights of shorter duration could become commonplace. As shown in Fig. 16, cutting the Earth-Moon transit time in half to ~36 hours will require the mission's total ΔV budget to increase by ~25% (from ~8 to 10 km/s). As a result, versatile LANTR engines with adequate supplies of LDP for refueling will be key to ensuring LTVs of reasonable size.

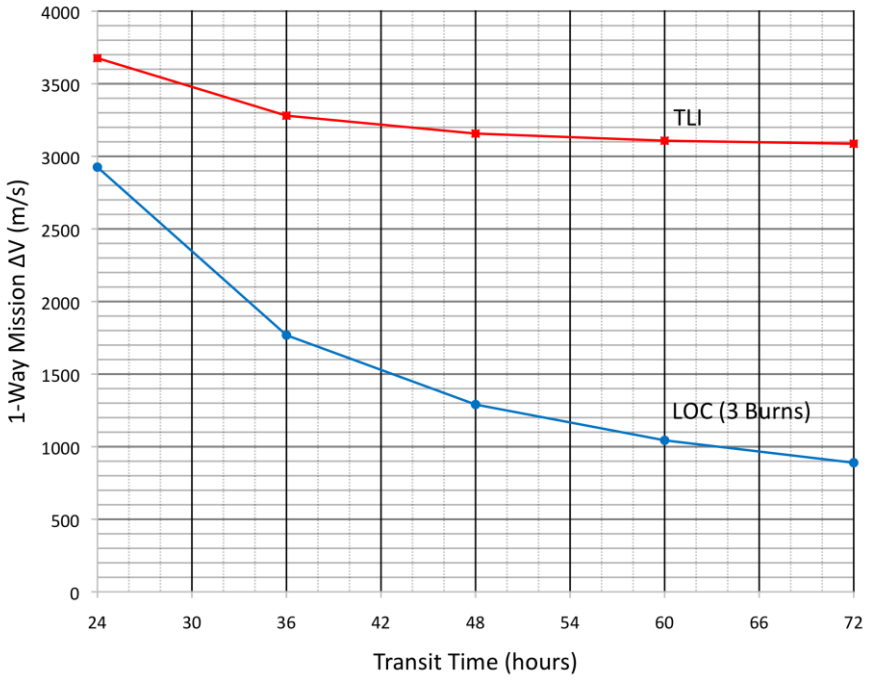

Figure 16. TLI and LOC ΔV Variation with Flight Time

VII. *Conestoga* - A Reusable, Space-based Crewed Cargo Transport

The original Conestoga wagon was a freight wagon developed in Lancaster County, Pennsylvania in the early 1700s [57] and used extensively in Pennsylvania and the nearby states of Maryland, Ohio and Virginia for more than 150 years. It was designed for hauling heavy loads – up to 6 tons – and had a distinctive bed that was curved upward at both ends to prevent the wagon's contents from shifting or falling out while traveling over rough roads. A white canvas cover protected the wagon's contents from inclement weather and a team of four to six strong horses pulled the wagon some 12 to 14 miles a day (shown in Fig. 17).

Figure 17. Conestoga Wagons, the "Ships of Inland Commerce," were used to Transport Settlers, Farm Produce, and Freight across Pennsylvania and Neighboring States (Image ca 1910) [58]

Named after its earlier ancestor, the *Conestoga* crewed cargo transport shown in Fig. 18 is a space-based, reusable LTV that uses LANTR propulsion and refuels with LDP. *Conestoga* has its own dedicated habitat module that supports a crew of 4 and has a mass of ~10 t. Two crewmembers operate the vehicle and manage the unloading of the PL. The other 2 represent rotating crewmembers on assignment at the lunar base or the LPO transportation node / propellant depot. Connecting the habitat module to the rest of the LANTR LTV is a 4-sided star truss that has four PL pallets attached to it – each weighing up to ~2.5 t. To accommodate the wedge-shaped geometry of the cargo pallets, the sides of the star truss are concave – a feature similar to the upward curving ends of the Conestoga wagon's bed though not for the same design reason. Attached to the star truss' forward circular ring is a RMS with twin arms that are free to move around the ring's outer perimeter (Fig. 18). Using the habitat module's rear viewing window, the crew uses these manipulator arms to unload and attach the *Conestoga's* cargo to either the depot node or to a co-orbiting LDAV transferring crew and awaiting cargo delivery. Key features and dimensions of the *Conestoga* are shown in Fig. 19 and major mission activities are shown in Fig. 20.

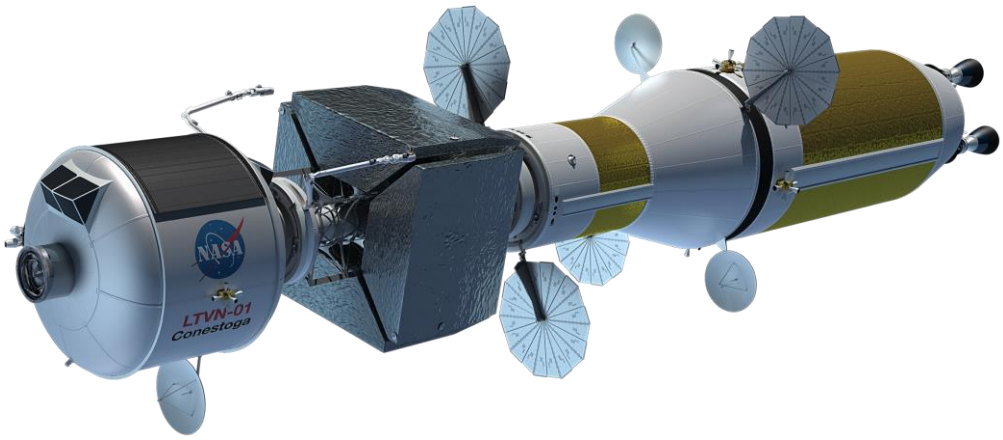

Figure 18. *Conestoga* - A Space-based Crewed Cargo Transport uses a Common NTPS and In-Line LO_2 Tank

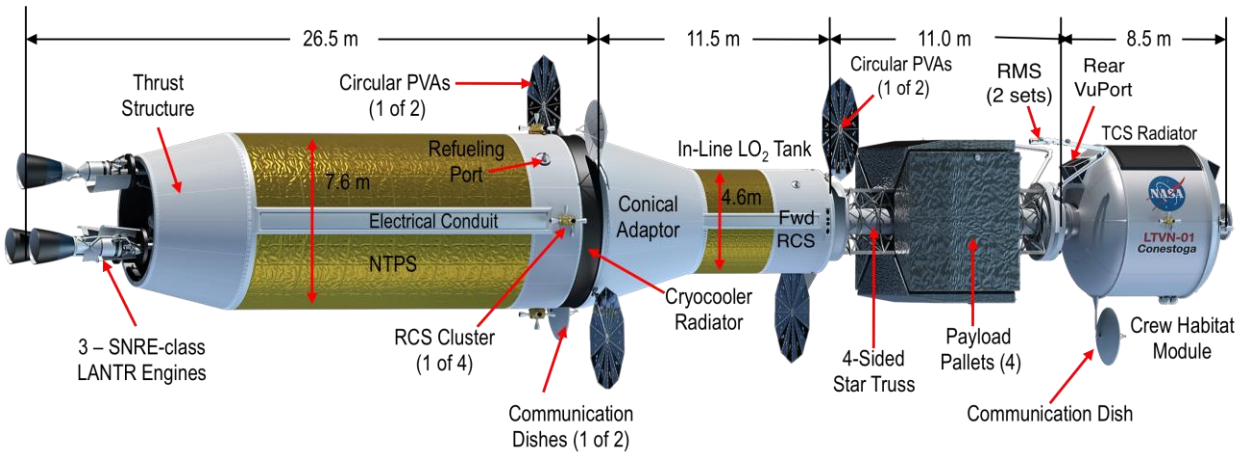

Figure 19. Key Features and Dimensions for the *Conestoga* Crewed Cargo Transport (CCT)

The *Conestoga* CCT is a versatile vehicle that can deliver varying amounts of cargo (from 10 to 40 t) to LPO depending on the transit times out and back. Once loaded with cargo at the LEO transportation node, the *Conestoga* leaves orbit for the Moon. After maneuvering into LPO, the *Conestoga's* cargo is then unloaded and attached to the LDAV using the vehicle's RMS as shown in Fig. 20. Outfitted with additional refueling appendages, the *Conestoga* can also function as a tanker vehicle capable of transferring ~9.4 t of LH_2 from it NTPS to the depot or supplying LH_2 propellant directly to the LDAV. Refueling ports and twin PVAs are located at the forward ends of both the NTPS and in-line LO_2 tank assembly for refueling in LEO and lunar orbit, and for powering the NTPS and forward PL element as shown in Fig. 19.

In this study, *Conestoga's* NTPS is limited to an ~70 t launch mass which includes ~39.8 t of LH_2 propellant. In a previous study [27] of LANTR-based LTVs operating out of equatorial LLO and using only LUNOX for refueling, *Conestoga's* LH_2 propellant loading was fixed so the outbound and return O/H MRs used by the LANTR engines were optimized to achieve the desired propulsion performance required to satisfy the particular mission objectives. Here, however, *Conestoga's* NTPS can top off its propellant tank with the excess LH_2 produced during the water electrolysis process. This ability to refuel with both LLO_2 and LLH_2 (albeit limited at an 8:1 ratio) provides an added degree of operational and mission flexibility not available to LANTR-based LTVs using LUNOX alone.

Figure 20. *Conestoga* Crewed Cargo Transport Mission - Outbound Leg and LPO Operations

Table 4. LANTR Crewed Cargo Missions, Trajectory and ΔV Budgets, and LDP Refueling Needs

Case Description *	Objective	Trajectory/Orbits **	In-line LO_2 Tank	Results
1. LANTR Crewed Cargo Transport with 9.9 t hab module and 11 m star truss carrying 10 t cargo to LLO	Determine LLO_2 refueling needed to deliver 10 t cargo to LLO while also cutting transit times to 36 hrs	36 hour 1-way transit times; LEO –– LLO – LEO ΔV ~9.920 km/s	4.6 m OD x ~7.95 m L (~111.2 t LO_2)	IMLEO ~214.3 t; ~111.2 t LO_2 supplied in LEO; ~75.0 t LLO_2 refueling in LLO
2. LANTR Crewed Cargo Transport with 9.9 t hab module and 11 m star truss carrying 10 t cargo to LPO	Determine the LLO_2 & LLH_2 refueling needed to deliver 10 t cargo to LPO while cutting transit times to 36 hrs	36 hour 1-way transit times; LEO – LPO – LEO ΔV ~10.115 km/s	4.6 m OD x ~7.95 m L (~111.2 t LO_2)	IMLEO ~215.2 t; ~111.2 t LO_2 supplied in LEO; ~50.5 t LLO_2 refueling in LPO ~6.32 t LLH_2 refueling in LPO
3. LANTR Crewed Cargo Transport with 9.9 t hab module and 11 m star truss carrying 10 t cargo to LPO	Minimize LEO LO_2 & LLO_2 refueling needed to deliver 10 t cargo to LPO and also cut transit times to 36 hrs	36 hour 1-way transit times; LEO –– LPO – LEO ΔV ~10.103 km/s	4.6 m OD x ~7.95 m L (~111.2 t LO_2)	IMLEO ~165.2 t; ~61.2 t LO_2 supplied in LEO; ~72.4 t LLO_2 refueling in LPO ~9.05 t LLH_2 refueling in LPO
4. LANTR Crewed Cargo Transport with 9.9 t hab module and two 11 m star trusses carrying 20 t cargo to LLO	Determine LLO_2 refueling needed to deliver 20 t of cargo to LLO with transit times of 72 hrs	72 hour 1-way transit times; LEO – LLO – LEO ΔV ~8.057 km/s	4.6 m OD x ~7.95 m L (~111.2 t LO_2)	IMLEO ~189.6 t; ~71.0 t LO_2 supplied in LEO; ~52.1 t LLO_2 refueling in LLO
5. LANTR Crewed Cargo Transport with 9.9 t hab module and two 11 m star trusses carrying 20 t cargo to LPO	Determine the LLO_2 & LLH_2 refueling needed to deliver 20 t cargo to LPO with transit times of 72 hrs	72 hour 1-way transit times; LEO – LPO – LEO ΔV ~8.097 km/s	4.6 m OD x ~7.95 m L (~111.2 t LO_2)	IMLEO ~232.2.1 t; ~111.2 t LO_2 supplied in LEO; ~25.6 t LLO_2 refueling in LPO ~3.20 t LLH_2 refueling in LPO
6. LANTR Crewed Cargo Transport with 9.9 t hab module and two 11 m star trusses carrying 20 t cargo to LPO	Minimize LEO LO_2 & LLO_2 refueling needed to deliver 20 t cargo to LPO with transit times of 72 hrs	72 hour 1-way transit times; LEO – LPO – LEO ΔV ~8.081 km/s	4.6 m OD x ~7.95 m L (~111.2 t LO_2)	IMLEO ~173.4 t; ~52.7 t LO_2 supplied in LEO; ~47.5 t LLO_2 refueling in LPO ~5.93 t LLH_2 refueling in LPO
7. LANTR Crewed Cargo Transport with 9.9 t hab module and two 11 m star trusses carrying 40 t cargo to LLO	Determine LLO_2 refueling needed to deliver 40 t of cargo to LLO with transit times of 72 hrs	72 hour 1-way transit times; LEO – LLO – LEO ΔV ~8.064 km/s	4.6 m OD x ~7.95 m L (~111.2 t LO_2)	IMLEO ~250.7 t; ~109.8 t LO2 supplied in LEO; ~60.3 t LLO_2 refueling in LLO
8. LANTR Crewed Cargo Transport with 9.9 t hab module and two 11 m star trusses carrying 40 t cargo to LPO	Determine the LLO_2 & LLH_2 refueling needed to deliver 40 t cargo to LPO with transit times of 72 hrs	72 hour 1-way transit times; LEO – LPO – LEO ΔV ~8.098 km/s	4.6 m OD x ~7.95 m L (~111.2 t LO_2)	IMLEO ~254.6 t; ~111.2 t LO2 supplied in LEO; ~37.5 t LLO_2 refueling in LPO ~4.69 t LLH_2 refueling in LPO
9. LANTR Crewed Cargo Transport with 9.9 t hab module and two 11 m star trusses carrying 40 t cargo to LPO	Minimize LEO LO_2 & LLO_2 refueling needed to deliver 40 t cargo to LPO with transit times of 72 hrs	72 hour 1-way transit times; LEO – LPO – LEO ΔV ~8.092 km/s	4.6 m OD x ~7.95 m L (~111.2 t LO_2)	IMLEO ~217.6 t; ~74.3 t LO2 supplied in LEO; ~57.2 t LLO_2 refueling in LPO ~7.15 t LLH_2 refueling in LPO

* Cases 1 – 9 use a "Common LH_2 NTPS" (7.6 m D x ~15.7 m L); Propellant depots assumed in LEO, LPO and LLO; LANTR engines use optimized MRs out and back
**LEO – 407 km, LPO – 300 km polar orbit, LLO – 300 km equatorial orbit; Total round trip mission ΔV values shown include g-losses

Table 4 provides a comparison of crewed cargo missions to LLO and LPO with different delivered payloads and trip times along with the associated IMLEO and LDP refueling requirements. All the cases shown use the same common NTPS and in-line LO_2 tank assembly as that shown in Figs 19 and 20. Case 1 shows the performance and refueling requirements for the baseline *Conestoga* CCT discussed in a previous study [27]. Operating between LEO and equatorial LLO, *Conestoga* was configured to deliver twice the PL (10 t) to LLO in half the time (36 hours instead of 72). To meet these demanding mission objectives with a fixed LH_2 propellant loading in its NTPS of ~39.8 t, *Conestoga's* in-line LO_2 tank is sized to hold ~111.2 t of LO_2 at mission start and its LANTR engines are operated "O_2-rich" on both the outbound mission leg (MR ~5, I_{sp} ~516 s for TLI; MR ~4.1, I_{sp} ~550 s for LOC) and return mission leg (MR ~5, I_{sp} ~516 s for both the TEI and EOC burns).

After dropping off its cargo and picking up 250 kg of lunar samples, *Conestoga* refuels with ~74.9 t of LLO_2 for the trip back to LEO. For this mission, *Conestoga* has an IMLEO of ~214.3 t consisting of the NTPS (~71 t), the in-line LO_2 tank and conical adaptor (~117.2 t), the star truss assembly with its RMS (~5.3 t) and attached PL (10 t), the habitat module (9.9 t), consumables (~0.1 t) plus the 2 crew and 2 passengers with their EVA suits (~0.8 t). The total mission ΔV to go from LEO to LLO and back again is ~9.92 km/s including g-losses. With the augmented thrust levels provided by the LANTR engines (~56.8 klb_f per engine at MR ~5), the burn times for the individual maneuvers are ~11.5 min (TLI), ~3.8 min (LOC), ~4.4 min (TEI), and ~5.6 min (EOC) totaling to ~25.3 minutes. *This total burn time is essentially fixed by the available amount of LH_2 in the NTPS and the LH_2 flow rate for each engine of ~8.3 kg/s. What varies in this case (as well as in Cases 4 and 7) is the amount of LO_2 supplied in LEO and LLO and the different MRs used by the LANTR engines to achieve the specified mission objectives.*

Case 2 shows the impact on *Conestoga* performance and refueling when operating out of LPO instead of LLO. With the ability to top off its NTPS with ~6.3 t of LLH_2, *Conestoga's* refueling requirements for the same mission scenario are reduced by ~18.2 t (~57 t of LLO_2 and LLH_2 versus ~75 t of LLO_2 when operating out of LLO and using only ELH_2). This reduction in refueling is the result of having top off LH_2 available that allows the LANTR engines to run at lower O/H MRs than Case 1 and therefore higher I_{sp} values on both the outbound and inbound mission legs. The IMLEO for this mission is ~215.2 t and the total mission ΔV is slightly larger at ~10.112 km/s. *The total mission burn time for Case 2 also increases to ~29.3 minutes – 4 minutes longer than in Case 1 since the LANTR engines now have more LH_2 available to use.*

As the mining and processing of LPI for propellant production increases, one might choose to minimize the total propellant requirements for the mission (both in LEO and LPO) by relying more heavily on LDPs especially if LEO launch costs remain high. Using this strategy, Case 3 illustrates that it is possible to reduce the amount of LEO-supplied LO_2 required for the same cargo delivery and mission trip time by ~45% – from ~111.2 t to ~61.2 t by leveraging the greater availability of LLO_2 and LLH_2 – in this case ~81.5 t at an 8:1 ratio. For this case, the *Conestoga's* LANTR engines run at low MRs on the outbound mission leg and O_2-rich on the inbound leg. The IMLEO for Case 3 drops by ~50 t to ~165.2 t but the total mission burn time increases to ~31.2 minutes – again due to the availability of additional LH_2 for the LANTR engines to use.

By extending 1-way transit times to 72 hours, Case 4 shows that a *Conestoga-class* vehicle can double the amount of cargo delivered to lunar orbit from 10 to 20 t. The *Conestoga-II*, shown in Fig. 21, is a heavy crewed cargo transport that adds a second 11 m star truss and RMS and four more 2.5 t PL pallets to the baseline vehicle configuration. This addition results in an increase in the vehicle's overall length from ~57.5 to ~68.5 m. Departing LEO with 71 t of LO_2, *Conestoga-II's* LANTR engines are run at an O/H MR of ~3.4 and I_{sp} of ~573 s. During LOC, the engines operate at low a MR of ~0.9 and I_{sp} at ~737 s. Once in orbit, the crew unloads the forward PL pallets first. This allows an unobstructed view of the rear PL section from the hab module's rear viewing port during the unloading process. After picking up samples, the *Conestoga-II's* LO_2 tank is refueled with ~52.1 t of LLO_2. On the return leg of the mission, the engines operate at MR ~4.7 and I_{sp} ~527 s during the TEI maneuver. For EOC, the engines operate at MR ~3.8 and I_{sp} ~558 s. The total mission ΔV is ~8.06 km/s, and the total burn time on the engines is ~25.3 minutes – again determined by the available amount of LH_2 in *Conestoga-II's* NTPS.

In Cases 5 and 6, the *Conestoga-II* operates out of LPO and is able to refuel with both LLO_2 and LLH_2. Case 5 minimizes LDP usage (~29 t) at the expense of an increased LEO LO_2 loading (~111.2 t) and IMLEO (~232.2 t). In Case 6, LDP usage is increased and the *Conestoga-II's* LANTR engines operate with low MR values outbound and higher values inbound. The result is a reduction in the amount of LEO-supplied LO_2 down to ~52.7 t and a decrease in the vehicle IMLEO to ~173.4 t. The amount of refuel LLO_2 and LLH_2 is ~53.4 t again supplied at an 8:1 ratio.

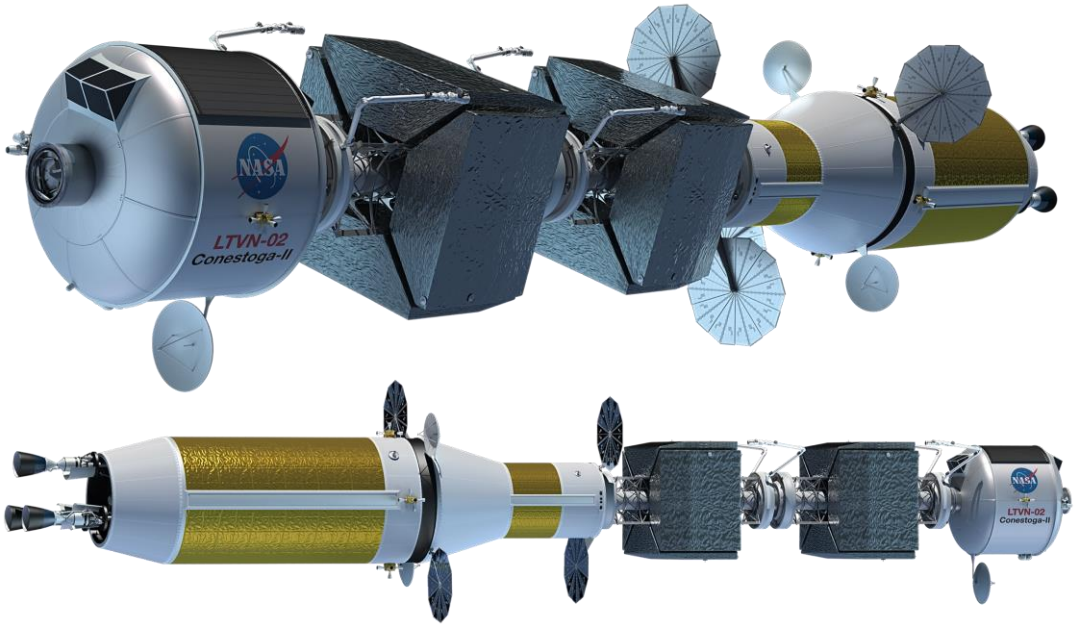

Figure 21. *Conestoga-II* Heavy Crewed Cargo Transport Isometric and Elevation

Case 7 pushes the *Conestoga-II's* cargo delivery capability to its limit for the amount of LH_2 and LO_2 propellant available in the NTPS and in-line LO_2 tank. Assuming 72-hour transit times, this limit is ~40 t (eight 5 t PL pallets). For this mission, the LO_2 loading at LEO departure is ~109.8 t (~98.5% of the tank's maximum capacity) and the LANTR engines are operated at MR ~4.4, I_{sp} ~536 s for TLI and MR ~3.3, I_{sp} ~578 s for LOC. On the return leg, the *Conestoga-II* is refueled with ~60.3 t of LLO_2 and its engines are operated at MR ~5, I_{sp} ~536 s for TEI and MR ~4.8, I_{sp} ~522 s for LOC. These MR conditions were selected by the optimizer to deliver the specified PL while also minimizing the total LO_2 requirement for the mission. The IMLEO for Case 7 is ~250.7 t and the total mission ΔV and engine burn time are ~8.06 km/s and ~25.3 minutes, respectively.

In Cases 8 and 9, the *Conestoga-II* delivers its 40 t PL to LPO and then refuels with both LLO_2 and LLH_2. Case 8 minimizes LDP usage (~42.2 t) at the expense of increased LEO LO_2 loading (~111.2 t) and IMLEO (~254.6 t). In Case 9, LDP usage is again increased leading to a reduction in LEO-supplied LO_2 down to ~74.3 t and a decrease in the vehicle IMLEO to ~217.6 t. The amount of refuel LLO_2 and LLH_2 used on the return mission leg is ~64.3 t and the total engine burn time is just short of 30 minutes.

The *Conestoga-class* CCTs shown departing LEO for the Moon in Fig. 22 can provide the basis for a robust and flexible LTS that offers a wide range of cargo delivery capability and transit times made possible through the use of LANTR propulsion and supplies of LDP provided at transportation nodes / propellant depots located in lunar orbit. Today, "time is money" for the long-distance freight haulers traveling our highways, oceans and skies. In the future, *Conestoga-class* vehicles could play the same important role in establishing cislunar trade and commerce as the Conestoga wagons of old did for more than a century throughout Pennsylvania and its neighboring states.

Figure 22. *Conestoga-class* Crewed Cargo Transports Departing LEO for the Moon

VIII. Commuter Shuttle Flights to the Moon

In the movie *2001: A Space Odyssey*, released by MGM in 1968 [59], Dr. Heywood Floyd departs from a huge artificial gravity space station orbiting Earth bound for the Moon. He arrives there 24 hours later [60] aboard a large spherical-shaped LTV called *Ares* which touches down on a landing pad that subsequently descends to a large sprawling lunar settlement located underground. Today, almost 50 years later, the images portrayed in Stanley Kubrick and Arthur C. Clarke's film remain well beyond our capabilities and *2100: A Space Odyssey* seems a more appropriate title for the movie. In this section, we evaluate the feasibility and requirements for commuter flights to the Moon using LANTR propulsion and LDP to see if the operational capabilities presented in *2001* can be achieved albeit on a more "Spartan" scale.

A 24-hour commuter flight to the Moon is a daunting challenge. This is about the time it now takes to fly from Washington, D. C. to Melbourne, Australia with a 3-hour layover in San Francisco. As Fig. 16 shows, decreasing the LEO-to-LPO transit time from 72 to 24 hours increases the outbound ΔV requirement from ~4 to 6.6 km/s and the total roundtrip ΔV requirement by ~5.2 km/s! Increasing the flight time from 24 to 36 hours each way decreases this additional ΔV requirement by ~3 km/s – down to ~2.2 km/s. Also, at these higher velocities, free return trajectories are no longer available so multiple engines will be required to improve reliability and increase passenger safety.

How might a typical commuter flight to the Moon proceed? A possible scenario might start with passengers boarding a future "Earth-to-Orbit" shuttle for a flight to a future International Space Station (ISS) shown in Fig. 23a. There they would enter a Passenger Transport Module (PTM) containing its own life support, power, instrumentation and control, and RCS. The PTM provides the "brains" for the LANTR-powered shuttle and is home to the 18 passengers and 2 crewmembers operating it while on route to the Moon. After departing the ISS (Fig. 23b), the PTM docks with the fully fueled LANTR shuttle awaiting it a safe distance away (shown in Fig. 24a). At the

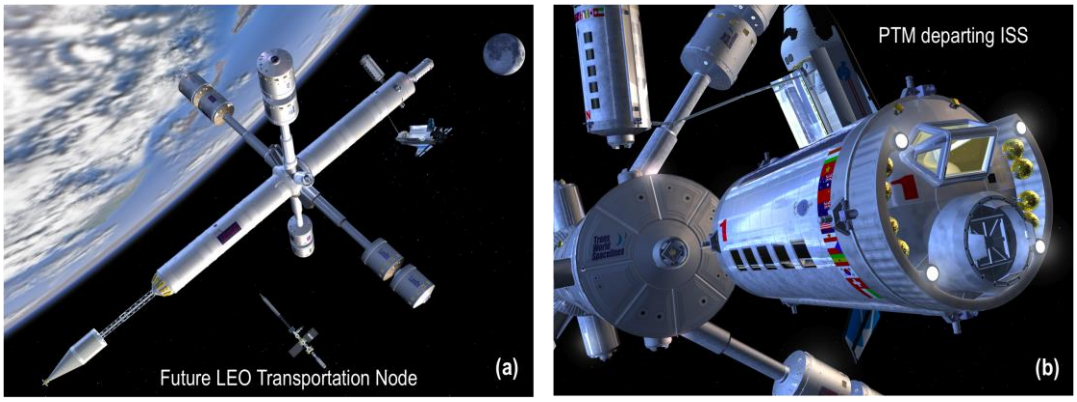

Figure 23. Future Commercial ISS Provides the Transportation Hub for PTMs Arriving and Departing from LEO

appropriate moment, the LANTR engines are powered up and the shuttle climbs rapidly away from Earth (Fig. 24b). For a 36-hour flight to the Moon, the acceleration experienced by the passengers during Earth departure will range from ~0.4 g_E to ~0.8 g_E near the end of the TLI burn.

Following the 36-hour transfer and insertion of the LANTR shuttle into lunar orbit, the PTM detaches and docks with a waiting "Sikorsky-style" LLV. A commercial propellant depot (shown in Fig. 15b) provides a convenient staging node for lunar orbit operations supplying the LANTR shuttle with LDP for Earth return and the LLV with Earth-supplied LH_2 needed to deliver the PTM to the lunar surface. From here the PTM is lowered to a "flat-bed" surface vehicle (shown in Fig. 24c) and electronically engaged providing the PTM with surface mobility. The PTM then drives itself to the lunar base airlock for docking and passenger unloading.

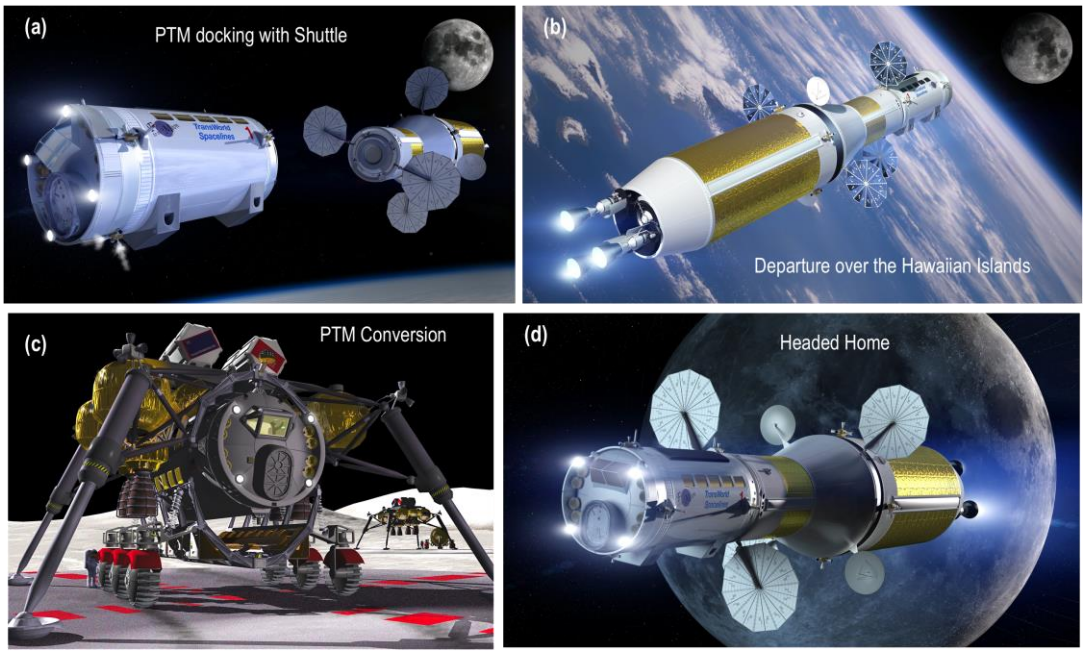

Figure 24. Various Phases of LANTR Commuter Shuttle Mission to the Moon

This scenario is reversed on the return trip to Earth (Fig. 24d). At the end of the flight, the passengers will also experience a bit of excitement as peak acceleration levels can reach ~1.4 g_E at the end of the LEO capture burn.

The commercial commuter shuttle we envision utilizes the same NTPS, LANTR engines, and in-line LO_2 tank assembly used on the *Conestoga* CCT shown in Fig. 19. For the commuter shuttle application, the CCT's habitat module, star truss and PL pallets are removed and replaced with a 20-person PTM (shown in Fig. 25). The fully loaded PTM has an estimated mass of ~15 t and its diameter and length are ~4.6 m by ~8 m, respectively.

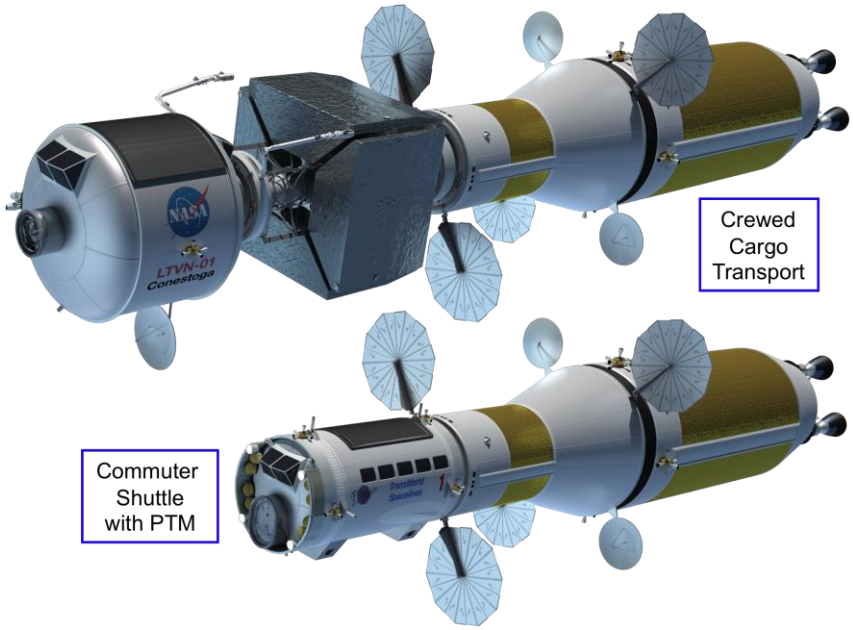

Figure 25. Relative Size of a CCT and Commuter Shuttle using a Common NTPS and In-Line LO_2 Tank Assembly

Table 5 provides a sampling of the different LANTR shuttle missions to LLO and LPO considered in this study. These missions looked at transit times ranging from 36 to 24 hours along with the associated LDP refueling requirements needed to achieve these trip times. Cases 1 through 4 use the same NTPS, clustered LANTR engines and in-line LO_2 tank assembly used on the *Conestoga-class* vehicles shown in Figs. 22. In Case 1, the PTM is transported to and from LLO with 1-way transit times of 36 hours. The code optimization feature is also used to minimize the LO_2 resupply in LEO by increasing the use of LLO_2 refueling for the return to Earth. Supplied with just over 76 t of LO_2 prior to TLI, the shuttle's engines operate at low MRs on the outbound leg (~3.9 for TLI and ~1.7 for LOC) requiring more LH_2 to be consumed. On the return leg, the LANTR engines operate O_2-rich (MR ~5 for TEI and ~4.9 for EOC) so the LLO_2 refueling requirement is ~72.8 t. The mission IMLEO is ~168.2 t and includes the NTPS (~71 t), the in-line LO_2 tank assembly and conical adaptor (~82.2 t), and the PTM (15 t). The total mission ΔV is ~9.914 km/s and the total engine burn time is ~25.3 minutes which includes the following individual burn times: ~10.5 min (TLI), ~5.0 min (LOC), ~4.3 min (TEI), and ~5.5 min (EOC).

Case 2 assumes the same 36-hour transit times but the shuttle now delivers the PTM to and from LPO instead of LLO and is able to refuel with both LLO_2 and LLH_2. In Case 1, the optimizer is used to minimize total LO_2 usage so the amount of LEO-supplied LO_2 is reduced to just under 41 t prior to TLI. For this mission, the LANTR engines run fuel-rich on the outbound leg and O_2-rich on the inbound leg after refueling with ~69.4 t of LLO_2 and ~8.67 t of LLH_2. The mission IMLEO is ~133.8 t and includes the NTPS (~71.3 t), the in-line LO_2 tank assembly and conical adaptor (~47.5 t), and the PTM (15 t). The total mission ΔV is ~10.109 km/s and the total engine burn time increases to ~30.9 minutes with additional top off LLH_2 to burn on the return mission leg.

Case 3 focuses on achieving the fastest transit times to and from LLO by taking full advantage of the extra propellant capacity that exists in the vehicle's in-line LO_2 tank. By increasing the commuter shuttle's LO_2 loading to its maximum capacity of ~111.2 t before TLI, refueling with ~80.4 t of LLO_2 before TEI, and operating the LANTR engines O_2-rich (MR ~5) out and back, the shuttle can decrease its 1-way transit time from 36 to 32.8 hours. The additional LO_2 loading prior to TLI increases the required IMLEO to ~203.3 t which includes the NTPS (~71 t), the in-line LO_2 tank assembly and adaptor section (~117.3 t), and the PTM (15 t). The decreased transit times increase

Table 5. LANTR Commuter Shuttle Options, Trip Time and ΔV Budgets, and LDP Refueling Needs

Case Description *	Objective	Trajectory/Orbits **	In-line LO_2 Tank	Results
1. LANTR commuter shuttle carrying 15 t Passenger Transport Module (PTM) to LLO then back to LEO	Minimize LEO LO_2 refueling needed to deliver the 15 t PTM to and from LLO with transit times of 36 hrs	36 hour 1-way transit times; LEO – LLO – LEO ΔV ~9.914 km/s	4.6 m OD x ~7.95 m L (~111.2 t LO_2)	IMLEO ~168.2 t; ~76.1 t LO_2 supplied in LEO; ~72.8 t LLO_2 refueling in LLO
2. LANTR commuter shuttle carrying 15 t PTM to LPO then back to LEO	Minimize LEO LO_2 and LLO_2 refueling needed to deliver the PTM to & from LPO with transit times of 36 hrs	36 hour 1-way transit times; LEO – LPO – LEO ΔV ~10.109 km/s	4.6 m OD x ~7.95 m L (~111.2 t LO_2)	IMLEO ~133.8 t; ~40.8 t LO_2 supplied in LEO; ~69.4 t LLO_2 refueling in LPO; ~8.67 t LLH_2 refueling in LPO
3. LANTR commuter shuttle carrying 15 t PTM to LLO then back to LEO	Determine LLO_2 refueling needed to deliver the PTM to and from LLO with shortest transit times possible	32.8 hour 1-way transit times; LEO – LLO – LEO ΔV ~10.481 km/s	4.6 m OD x ~7.95 m L (~111.2 t LO_2)	IMLEO ~203.3 t; ~111.1 t LO_2 supplied in LEO; ~80.4 t LLO_2 refueling in LLO
4. LANTR commuter shuttle carrying 15 t PTM to LPO then back to LEO	Determine LLO_2 and LLH_2 refueling needed to deliver the PTM to & from LPO with shortest transit times	25.6 hour 1-way transit times; LEO – LPO – LEO ΔV ~12.519 km/s	4.6 m OD x ~7.95 m L (~111.2 t LO_2)	IMLEO ~204.8 t; ~111.2 t LO_2 supplied in LEO; ~106.4 t LLO_2 refueling in LPO ~13.30 t LLH_2 refueling in LPO
5. LANTR commuter shuttle with 2 engine NTPS and carrying 15 t PTM to LLO then back to LEO	Determine LLO_2 refueling needed to deliver the PTM to and from LLO with shortest transit times possible	30.3 hour 1-way transit times; LEO – LLO – LEO ΔV ~11.107 km/s	4.6 m OD x ~7.95 m L (~111.2 t LO_2)	IMLEO ~197.7 t; ~111.2 t LO_2 supplied in LEO; ~79.0 t LLO_2 refueling in LLO
6. LANTR commuter shuttle with 2 engine NTPS and carrying 15 t PTM to LPO then back to LEO	Determine LLO_2 and LLH_2 refueling needed to deliver the PTM to & from LPO with transit times of 24 hrs	24 hour 1-way transit times; LEO – LPO – LEO ΔV ~13.304 km/s	4.6 m OD x ~8.45 m L (~119.5 t LO_2)	IMLEO ~207.6 t; ~119.5 t LO_2 supplied in LEO; ~106.0 t LLO_2 refueling in LPO ~13.25 t LLH_2 refueling in LPO

* Cases 1 – 6 use a "Common LH_2 NTPS" (7.6 m D x ~15.7 m L); Propellant depots assumed in LEO, LPO and LLO; LANTR engines use optimized MRs out and back
**LEO – 407 km, LPO – 300 km polar orbit, LLO – 300 km equatorial orbit; Total round trip mission ΔV values shown include g-losses

the total mission ΔV by ~0.567 km/s to ~10.5 km/s. The total mission burn time is ~25.3 minutes and the individual burn times are ~11 min (TLI), ~3.5 min (LOC), ~5.1 min (TEI), and ~5.7 min (EOC).

Case 4 is also focused on achieving the fastest transit times but to and from LPO instead of LLO. Like Case 3, the commuter shuttle's LO_2 tank is filled to its maximum capacity of ~111.2 t before TLI. It then refuels with ~119.7 t of LLO_2 and LLH_2 and operates its engines O_2-rich (MR ~5) on the trip back to LEO, enabling the shuttle to decrease its 1-way transit time from 36 to 25.6 hours. The additional LO_2 loading prior to TLI and the higher total mission ΔV (~12.5 km/s) increases the shuttle's IMLEO to ~204.8 t. The extra refueling with top off LLH_2 also increases the total burn time on the engines to ~33.9 minutes.

Case 5 and 6 differ from the first 4 in that the shuttle uses only two LANTR engines instead of three thereby decreasing the dry mass of its NTPS by ~5.5 t – the mass of the engine, its external radiation shield and thrust vector control system. By reducing the NTPS mass, the shuttle's transit times to and from LLO and LPO can be shortened even further. In Case 5, the shuttle is again supplied with ~111.2 t of LO_2 before TLI, refuels with ~79 t of LLO_2 in LLO, and operates its engines O_2-rich out and back allowing 1-way transit times of ~30.3 hours. The IMLEO for this case is ~197.7 t that includes the NTPS (~65.5 t), the in-line LO_2 tank assembly and adaptor section (~117.2 t), and the PTM (15 t). The decreased transit time increases the total mission ΔV to ~11.1 km/s including the increased g-losses that occur from using only two engines. *With the available LH_2 and one less engine, the maximum mission burn time increases from ~25.3 to 37.9 minutes.* The individual burn durations are ~16.5 min (TLI), ~5.6 min (LOC), ~8 min (TEI), and ~7.8 min (EOC).

Case 6 uses a larger LO_2 tank and operates out of LPO instead of LLO. By supplying the shuttle with ~119.5 t of LO_2 prior to TLI, refueling it with ~106 t of LLO_2 and ~13.2 t of LLH_2, and operating the LANTR engines O_2-rich on the way back to Earth, the 24-hour trip to the Moon taken by Dr. Floyd in *2001* becomes a possibility. The IMLEO for this case is ~207.6 t which includes the NTPS (~66.2 t), the in-line LO_2 tank assembly and its adaptor (~126.4 t), and the PTM (15 t). The total ΔV required for this rapid shuttle capability to the Moon is ~13.3 km/s. *With additional LH_2 supplied to the NTPS but only two engines to use it, the total mission burn time on the engines increases to ~50.8 minutes* with burn times of ~18.7 min (TLI), ~10.9 min (total LOC), ~12.4 min (total TEI), and ~8.8 min (EOC). Although the fastest shuttle option, Case 6 has a number of negative features when compared to Cases 3 and 4: (1) it has the largest IMLEO; (2) requires significant LPO refueling; (3) has the largest total ΔV; and (4) total burn time requirement; and (5) has a less robust "engine-out" capability with only 2 engines.

IX. Mining and Processing Requirements and estimated LDP Reserves

In the last two sections of this paper, two different options for obtaining and using LDP were discussed and compared. The first option produces LLO_2 or LUNOX from abundant volcanic glass deposits, and the second option produces both LLO_2 and LLH_2 from LPI deposits. In Option 1, we assume the LLO depot is routinely supplied with LUNOX transported from the surface by reusable tanker LLVs. In Option 2, we assume the tanker LLVs transport H_2O to the LPO depot where it electrolyzed and stored for subsequent use.

Because of water's composition (8:1 O/H mass ratio), ~1.125 tons of water must be produced and electrolyzed for every ton of LLO_2 required for LTV refueling. Additional water must also be produced to supply the LDP the tanker LLVs need to deliver water to the depot. Because the LLVs use LO_2/LH_2 chemical rockets operating at an O/H MR of ~6, it will be necessary to overproduce on water to supply the required amounts of LH_2 needed by the LLVs unless supplemental ELH_2 is supplied to the depot for their use. The required electrolysis power (in kW_e) is ~4.9 x H_2O electrolysis rate (in kg/hr), so once the quantities of water needed on the lunar surface and at the orbital depot are established for the different mission types and their frequency, the required power levels at these locations can be partly determined. *An estimate of the total power requirement will need to include mining, transportation of the ice-bearing regolith to the processing plant, water extraction and cleanup, storage and eventual electrolysis*.

As discussed in Sect. II, there are still many unknowns and many questions that need to be answered about LPI mining and use before total system mass and power estimates can be made. For example, what is the water content of the ice-bearing regolith and can it be excavated? What kind of mining equipment is needed? Can it be operated in the deep cold, permanently dark polar craters without breaking? Does the equipment need to be heated in order to work, or can the surface material be warmed in advance using microwaves or infrared heaters in front of the mining equipment, or will both be required? Is the regolith processed within the crater or outside and by what means? What power source will be used – nuclear fission or high availability solar photovoltaic arrays located at the crater rims?

By contrast, the viability of producing LUNOX from samples of ilmenite and FeO-rich volcanic glass returned on earlier Apollo missions has been demonstrated experimentally using the hydrogen reduction process [21,22] and a detailed concept design study of a LUNOX production facility using this process has also been produced [31]. To get an idea what the mining and processing requirements are to support the kinds of missions discussed in this paper, we selected the 3-engine LANTR commuter shuttle mission to LLO (Case 3 in Table 5) that operates O_2-rich out to the Moon and back, and has 1-way transit times of ~32.8 hours. The LUNOX refueling requirement for this mission is ~80.5 t and the total mission burn time on each of the LANTR engines is ~25 minutes. Assuming a 10 hour "full-power" lifetime on the engine fuel, a typical LANTR shuttle could perform ~24 missions. Assuming a 5-ship fleet and weekly trips to the Moon, each LANTR shuttle would make around 10 to 11 flights per year resulting in a service life of ~2.2 years. Near the end of life, the shuttle's NTPS would be refueled then used to inject cargo to various destinations before being disposed of in heliocentric space.

To support weekly commuter flights to the Moon will require annual LUNOX production levels of ~12,540 t/yr (see Table 6). Approximately 4,190 t of LUNOX is used by the LANTR shuttle, ~6,140 t by four second generation Sikorsky-style LUNOX tanker LLVs (see Fig. 26) flying one resupply mission to the LLO depot each week over the

Table 6. Total LUNOX Required for "Weekly" Commuter Flights

32.8 Hour "1-Way" Transits (15 t / 20 Person PTM):	
LANTR Shuttle: (80.5 t LUNOX /mission/week) x 52 weeks/year	= 4,186 t/yr
LLV*+ : (29.5 t LUNOX / flight+) x (1 flight/LLV/week) x 4 LLVs x 52 weeks/year	= 6,136 t/yr
LLV*# : (42.7 t LUNOX# / round trip flights / week) x 52 weeks /year	= 2,220 t/yr
Total LUNOX Rate	= 12,542 t/yr

* O/H MR = 6, I_{sp} = 465 s, ΔV_{desc} = 2000 m/s and ΔV_{asc} = 1900 m/s assumed
+LLV tanker transports ~25 t of LUNOX to LLO; returns to LS with empty 5 t tank
#Total for LLV delivery of PTM from LLO to LS plus the PTM return from the LS to LLO

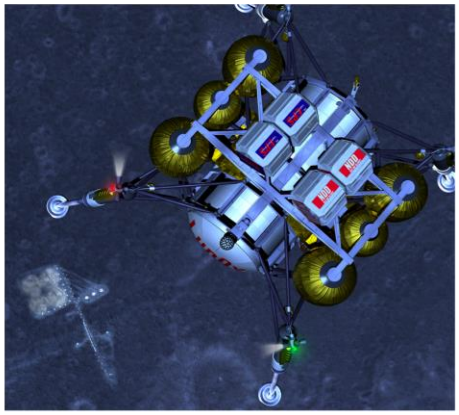

Figure 26. Tanker LLV Delivering LUNOX to LLO Depot

course of a year, and ~2,220 t used by the same Sikorsky-style LLVs to transport arriving and departing PTMs to and from the LS. Each LLV has a dry mass of ~10.9 t and a maximum LH_2/LO_2 propellant capacity of ~35 t.

A preliminary assessment of plant mass, power level, feedstock throughput, and required mining area has been made assuming a LUNOX operation employing thirteen modular units each with a production capacity of 1000 t/yr. Table 7 compares the characteristics for two LUNOX plants – one based on hydrogen reduction of ilmenite [31], and the other on "iron-rich" volcanic glass [27]. The advantages of using volcanic glass feedstock are apparent and show mass and power requirements that are 43% and 50% lower than that of an ilmenite reduction plant using soil feedstock. Included in the volcanic glass reduction plant mass of ~105.3 t is the mining (~9.6 t) and processing equipment (84.6 t) – both of which include a 30% DWC – plus the fission reactor power source (~11.1 t). The plant power requirement of ~1.52 MW_e includes ~10.7 kW_e for the mining equipment and ~1509 kW_e for the processing equipment. Both values again include a 30% margin. The process power dominates and is a function of the LUNOX production rate and is primarily associated with the electric heaters, electrolysis cell and the oxygen liquifiers.

Using the "low end" 4% O_2 yield obtained from orange and black volcanic glass beads still translates into more than an order of magnitude reduction in the amount of mined material. The mining equipment used at each 1000 t/yr production plant consists of two front-end loaders and four haulers. To produce ~13,000 t of LUNOX annually will require a glass throughput of ~3.25 x 10^5 t/yr and a soil mining rate at each production plant of just under 6 t per hour per loader assuming the same 35% mining duty cycle used in the ilmenite processing plant results. *This duty cycle corresponds to mining operations during ~70% of the available lunar daylight hours (~3067 hours per year).*

While this number is large, it is modest compared to terrestrial coal and proposed lunar helium-3 mining activities. For example, with a single 1000 MW_e coal-fired power plant consuming about sixty 100-ton train cars of coal per day, the annual U.S. production rate for coal exceeds 500 million tons! Similarly, past proposals for mining helium-3 on the Moon [61] to support a future fusion-based power economy in the U.S. would require the processing of ~2.8 billion tons of regolith to obtain the estimated 20 t of helium-3 needed annually (see Table 7).

Table 7. Comparison of Different Lunar Mining Concepts Showing Plant Mass, Required Operating Power, and Mining Rates

• Hydrogen Reduction of Ilmenite: (LUNOX Production @ 1000 t/year)	
• Plant Mass (Mining, Beneficiation, Processing and Power)	= 244 t
• Power Requirements (Mining, Beneficiation and Processing)	= 3.0 MW_e
• Regolith Throughput (assumes soil feedstock @ 7.5 wt% ilmenite and mining mass ratio (MMR) of 327 t of soil per ton of LUNOX)	= 3.3x10^5 t/yr
• Hydrogen Reduction of "Iron-rich" Volcanic Glass: (LUNOX Production @ 1000 t/year)	
• Plant Mass (Mining, Processing and Power)	= 105 t
• Power Requirements (Mining and Processing)	= 1.5 MW_e
• Regolith Throughput (direct feed and processing of "iron-rich" volcanic glass beads assuming a 4% O_2 yield and MMR = 25 to 1)	= 2.5x10^4 t/yr
• Lunar Helium-3 Extraction: (5000 kg (5 t) He^3/year)	
• Mobile Miners (150 miners required, each weighing 18 t, and each miner producing 33 kg He^3 per year)	= 2700 t
• Power Requirements (200 kW direct solar power/miner)	= 30.0 MW
• Regolith Throughput (processing and capture of Solar Wind Implanted (SWI) volatiles occurs aboard the miner)	= 7.1x10^8 t/yr

Figure 27 shows our proposed site for a commercial LUNOX facility within the Taurus-Littrow DMD at the southeastern edge of the Mare Serenitatis (~21°N, ~29.5°E) approximately30 km west of the Apollo 17 landing site. This deposit of largely black crystalline beads covers ~3000 km^2 and is thought to be tens of meters thick. Assuming an area of ~2000 km^2 – equivalent to a square ~28 miles on a side, a mining depth of ~5 m, a soil density for the volcanic glass of ~1.8 g/cm^3, and a MMR of 25 to 1 (equivalent to a 4% O_2 yield), Fig. 28 shows that the Taurus-Littrow DMD could produce ~720 million tons of LUNOX. Figure 28 also shows that the mining areas needed to support commuter flights to the Moon are not unrealistic at ~0.036 km^2 and ~0.18 km^2 for 1 to 5 flights/week, respectively. Even at five times the higher ~65,000 t/year rate, there are sufficient LUNOX resources at this one site to support ~25 commuter flights carrying 450 passengers each week for the next 2215 years and more sites containing even larger quantities of iron-rich pyroclastic glass have been identified [24].

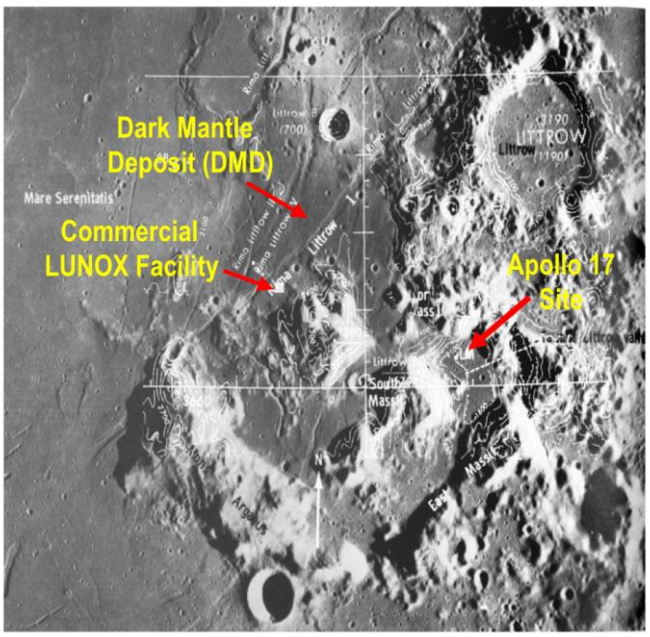

Figure 27. Apollo 17 Site and Major Geographic Features of the Taurus-Littrow Region

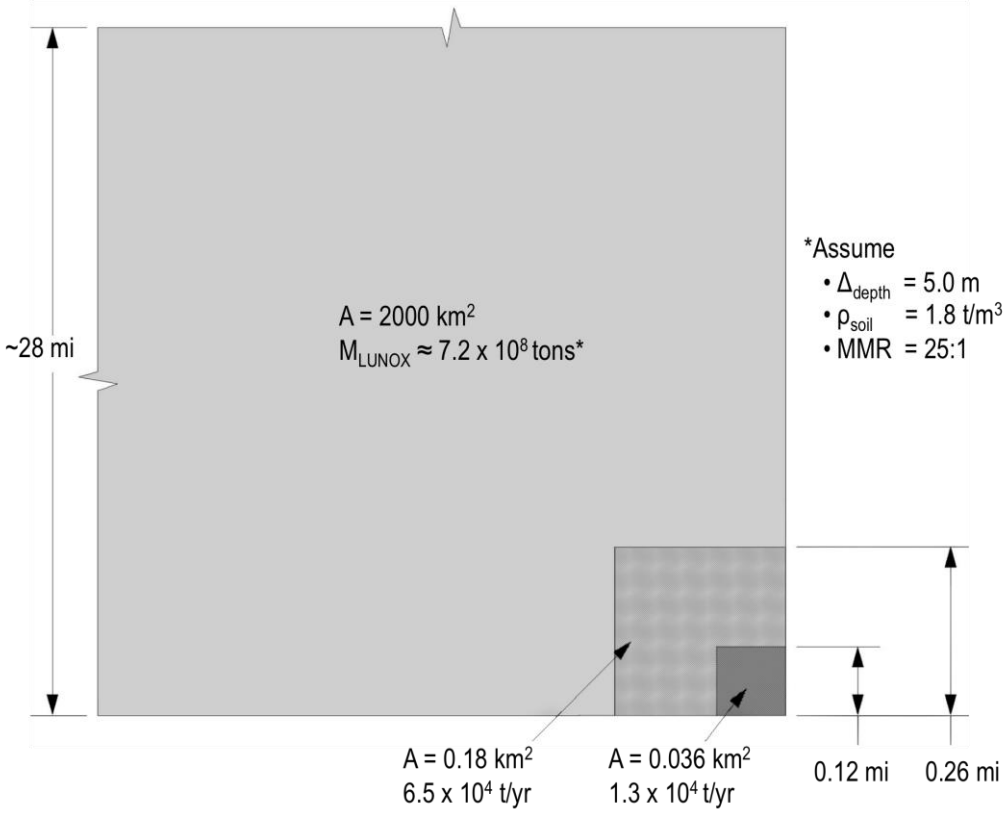

Figure 28. Required Mining Areas and LUNOX Production Rates to Support Routine Commuter Flights to the Moon

X. Summary, Concluding Remarks and a Look Ahead

The use of LDPs – specifically LLO_2 and LLH_2 from LPI or LUNOX from volcanic glass – offers substantial mission leverage when used with a compatible propulsion system. Although LUNOX is a much more established option, the use of LPI-derived propellant has received considerable attention. In this paper, we have tried to point out some of the issues that will need to be considered in the mining and processing of LPI for water and its subsequent conversion to LO_2 and LH_2 propellant. Spudis and Lavoie [25] assumed a 10 wt% water concentration in the polar regolith and relatively lightweight mining and processing equipment in their analysis of how lunar resources can be used to support the development of a cislunar space transportation system. However, the extreme environment in which the LPI exists is expected to pose significant engineering challenges to equipment operation. As pointed out by Gertsch et al. [50,51] at an ~10 wt% water ice content, ice-cemented regolith could behave like high strength concrete and require much heavier equipment for its excavation.

The design and engineering of systems for mining and processing volcanic glass is also expected to be challenging. Since a lunar day is ~29.53 days long, daytime on the Moon lasts ~14.76 days followed by ~14.76 days of lunar darkness. On the lunar nearside near the equator, where the vast deposits of volcanic glass are located, the temperature can vary from a low of ~95 °K (~ -178 °C) just before lunar sunrise to a high of ~392 °K (~119 °C) at lunar noon [62]. By contrast, in the depths of the permanently dark polar craters where the water ice is located, the temperature is ~2-3x colder than the coldest temperature on the lunar nearside and is unrelenting.

The main problems with mining volcanic glass are equipment cooling during the lunar day and heating during the lunar night. Illuminating the mine site during the lunar night can also require a large amount of power. In the study by Christiansen et al. [31], ilmenite mining was limited to the lunar daytime and a 35% duty cycle was assumed corresponding to mining operations during ~70% of the available lunar daylight hours (~3067 hours per year). A nuclear fission power source allowed the processing plant to operate both day and night with a 90% duty cycle. *A similar detailed study on the mining and processing of LPI will be required to help define the most viable concepts and systems, and to quantify the associated mass and power levels that will be needed for a LPI mining operation.*

The NTR also offers significant benefits for lunar missions and can take advantage of the mission leverage provided from using LDP by transitioning to LANTR propulsion. Using this enhanced version of NTP has many advantages. It provides a variable thrust and I_{sp} capability, shortens engine burn times, extends engine life and allows bipropellant operation. Its use together with adequate supplies of LDPs – extracted from either abundant reserves of volcanic glass or LPI, can lead to a robust nuclear LTS that evolves over time and has unique mission capabilities. The examples we have discussed here include short transit time crewed cargo transports and commuter shuttles operating between transportation nodes/propellant depots located in LEO, LLO and LPO. While others have discussed more conventional space transportation systems supported by strategically located propellant depots [63], the performance capability resulting from combining the two "high leverage" technologies discussed in this paper is quite extraordinary. To illustrate this fact more clearly, if one were to perform the same 36-hour commuter shuttle mission with the same propellant tank volumes used in Case 1 of Table 5, an all LH_2 NTP system would require an "effective I_{sp}" of ~1575 s which is equivalent to that postulated for an advanced "gaseous fuel core" NTR system.

Besides enabling a robust and versatile LTS, the LANTR concept is expected to dramatically improve space transportation performance wherever extraterrestrial sources of LO_2 and LH_2 can be acquired (Fig. 29) such as the Martian system, main-belt asteroids and the Galilean satellites – Europa, Ganymede, and Callisto.

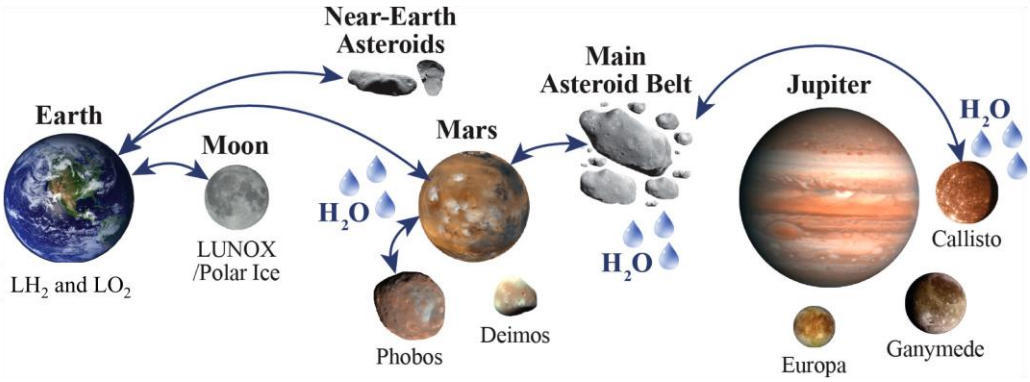

Figure 29. Human Expansion Possibilities using LANTR Propulsion and Extraterrestrial Propellant Resources

In the future, reusable biconic-shaped LANTR-powered ascent/descent vehicles, operating from specially prepared landing sites on Mars, could be used to transport modular payload elements to the surface and resupply interplanetary transfer vehicles (ITVs) with the propellants (shown in Fig. 30) needed to reach refueling depots in the asteroid belt. From there, LANTR-powered ITVs, carrying cargo and passengers, could continue on to the "water-rich" moons of the Jovian system, providing a reliable foundation for the development and eventual human settlement of the Solar System.

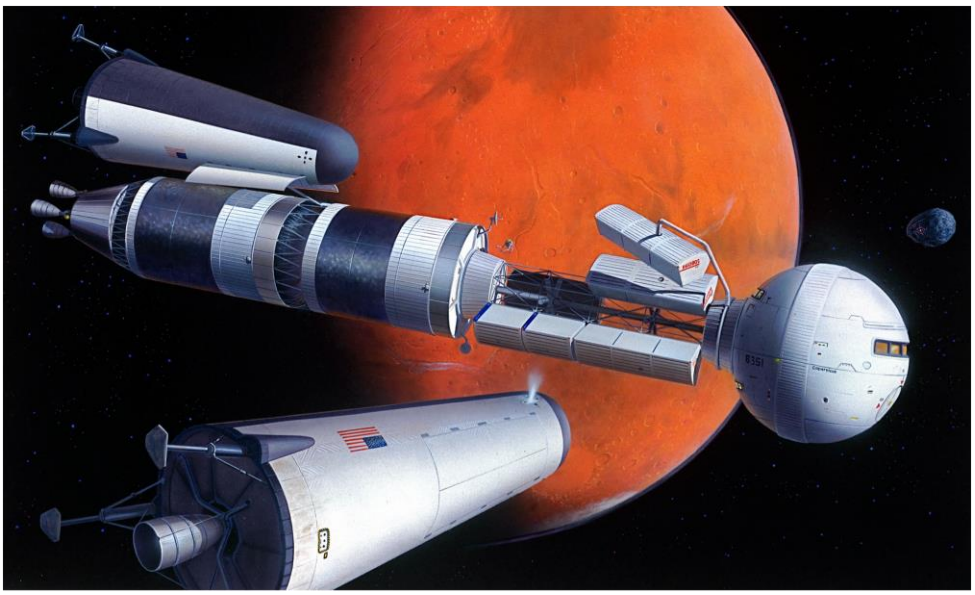

Figure 30. Notional LANTR-powered ITV Unloading Cargo and Loading Propellant before Departing Mars for the Asteroid Belt

This December marks the 45th anniversary of the Apollo 17 mission to Taurus-Littrow and unfortunately, the termination of both the Apollo and the Rover/NERVA nuclear rocket programs. In the not-so-distant future, the technological progeny from these two historic programs – LANTR and LDP – could allow the development of a robust, reusable space transportation system that can be adapted to a wide variety of potential lunar missions using the basic vehicle building blocks discussed in this paper.

After developing NTP and the oxygen afterburner nozzle for LANTR, the next biggest challenge to making this vision of a robust LTS a reality will be the production of increasing amounts of LDP and the development of propellant depots for vehicle refueling in LEO, LLO and/or LPO. An industry-operated, privately-financed venture, with NASA as its initial customer, has frequently been mentioned as a possible blueprint for how a commercial lunar propellant production facility and orbital depot might develop. With industry interested in developing cislunar space and commerce, and competitive forces at work, the timeline for developing this capability could well be accelerated beyond anything currently being envisioned. Only time will tell and maybe it will be quicker than any of us can imagine.

Acknowledgments

The author (SKB) acknowledges the NTP Project, the Nuclear Power and Propulsion Technical Discipline Team (NTDT), and Mark Klem (GRC Branch Chief) for their support of this work. Informative exchanges with Carlton Allen, Leslie Gertsch and Jerry Sanders are also acknowledged. The author also expresses his thanks to two outstanding space artists – Bob Sauls (bob.sauls@xp4d.com) and Pat Rawlings (pat@patrawlings.com) – whom he has had the pleasure of working with over the course of his 29-year career at NASA. Their work has helped bring the vehicle designs and missions developed and proposed by the author to life. The NASA-funded images produced by Pat include Figs. 1a-b, 15a-b, 23a-b, 24c, 26 and 30, and those by Bob include Figs. 1c-e, 5, 10-14, 18-22, 24a, b and d, and 25.

References

[1] NASA's Journey to Mars – Pioneering Next Steps in Space Exploration, National Aeronautics and Space Administration, NP-2015-08-2018-HQ, Washington, DC, October 2015.

[2] Achenbach, J., "Trump, with NASA, has a new rocket and spaceship. Where's he going to go?," *The Washington Post*, Health & Science, March 12, 2017; www.washingtonpost.com/national/health-science/trump-with-nasa...

[3] David, L., "Lunar Leap: Europe is Reaching for a Moon Base by the 2030s," Space.com, December 30, 2015; www.space.com/31488-european-moon-base-2030s.html.

[4] Aliberti, M., *When China Goes to the Moon*, ESPI, Springer Wien, New York, 2015.

[5] Zolfagharifard, E., and Gray, R., "Russia to Conquer the Moon in 2030: Country says it's planning a permanent manned base on the lunar surface," Daily Mail, December 3, 2015; www.dailymail.co.uk/sciencetech/article-3344818/Russia.

[6] Chang, K., "SpaceX Plans to Send 2 Tourists Around the Moon in 2018," *The New York Times*, Science, February 27, 2017; www.nytimes.com/2017/02/27/science/spacex-moon-tourists.html.

[7] Malik, T., "Private Space Stations Could Orbit the Moon by 2020, Robert Bigelow says," Space.com, March 9, 2017; www.space.com/35978-private-moon-refueling-station-by-2020.html.

[8] Wall, M., "Mining the Moon's Water: Q&A with Shackleton Energy's Bill Stone," Space.com, January 13, 2015; www.space.com/10619-minimg-moon-water-bill-stone-110114.html.

[9] David, L., "Inside ULA's Plan to Have 1,000 People Working in Space by 2045," Space.com, June 29, 2016; www.space.com/33297-satellite-refueling-business-proposal-ula.html.

[10] Davenport, C., "An exclusive look at Jeff Bezos's plan to set up Amazon-like delivery for 'future human settlement' of the moon," *The Washington Post*, The Switch, March 2, 2017; www.washingtonpost.com/news/the-switch//wp/2017/03/02/an-exclusive…

[11] Sullivan, T. S., and McKay, D. S., Using Space Resources, NASA Johnson Space Center, pp. 4, 1991.

[12] Allen, C. C., Morris, R. V., and McKay, D. S., "Experimental Reduction of Lunar Mare Soil and Volcanic Glass," *Journal of Geophysical Research*, 99, pp. 23,173-23,185, November 1994.

[13] http://nssdc.gsfc.nasa.gov/planetary/ice/ice_moon.html, "Ice on the Moon - A Summary of Clementine and Lunar Prospector Results," December 10, 2012.

[14] Borowski, S. K., "The Rationale/Benefits of Nuclear Thermal Rocket Propulsion for NASA's Lunar Space Transportation System," AIAA-91-2052, June 1991 (also NASA TM – 106730).

[15] Borowski, S. K., and Alexander, S. W., "Fast Track NTR Systems Assessment for NASA's First Lunar Outpost Scenario," AIAA-92-3812, July 1992 (also NASA TM – 106748).

[16] Borowski, S. K., McCurdy, D. R., and Burke. L. M., "The Nuclear Thermal Propulsion Stage (NTPS): A Key Space Asset for Human Exploration and Commercial Missions to the Moon," AIAA–2013-5465, September 2013 (also NASA/TM–2014-218105).

[17] Borowski, S. K., et al., "Affordable Development and Demonstration of a Small Nuclear Thermal Rocket (NTR) Engine and Stage: How Small is Big Enough?," AIAA–2015-4524, August 31–September 2, 2015 (also NASA/TM–2016-219402).

[18] Borowski, S. K., and Dudzinski. L. A., "*2001: A Space Odyssey* Revisited – The Feasibility of 24 Hour Commuter Flights to the Moon Using NTR Propulsion with LUNOX Afterburners," AIAA–97-2956, July 1997 (also NASA/TM–1998-208830/REV2).

[19] Joyner, C. R., et al., "TRITON: A *Tri*modal capable, *T*hrust *O*ptimized *N*uclear Propulsion and Power System for Advanced Space Missions," AIAA–2004-3863, July 2004.

[20] Bulman, M. J., et al., "LANTR Engine System Integration," AIAA–2004-3864, July 2004.

[21] Allen, C. C., and McKay, D. S., "Lunar Oxygen Production -- Ground Truth and Remote Sensing," AIAA 95-2792, July 1995.

[22] Allen, C. C., Morris, R. V., and McKay, D. S., "Oxygen Extraction from Lunar Soils and Pyroclastic Glass," *Journal of Geophysical Research*, 101, pp. 26,085-26,095, November 1996.

[23] Hawke, B. R., Coombs, C. R., and Clark, B., "Ilmenite-rich Pyroclastic Deposits: An Ideal Lunar Resource," in proceedings of *20th Lunar and Planetary Science Conference*, Houston, pp. 249-258, 1990.

[24] Gaddis, L. R., et al., "Compositional analyses of lunar pyroclastic deposits," *Icarus*, 161, pp. 262-280, 2003.

[25] Spudis, P. D., and Lavoie, A. R., "Using the resources of the Moon to create a permanent, cislunar space faring system," AIAA–2011-7185, September 2011.

[26] Haruyama, J., et al., "Lack of Exposed Ice Inside Lunar South Pole Shackleton Crater," *Science*, 322, pp. 938-939, November 7, 2008.

[27] Borowski, S. K., et al., "Robust Exploration and Commercial Missions to the Moon Using LANTR Propulsion and Lunar Liquid Oxygen Derived from FeO-rich Pyroclastic Deposits," AIAA–2017-4938, July 2017.
[28] Davis, H. P., "Lunar Oxygen Impact upon STS Effectiveness," Eagle Engineering Report No. 8363, Eagle Engineering, Inc., Houston, Texas, May 1983.
[29] Frisbee, R. H., and Jones, R. M., "An Analysis of Propulsion Options for Transport of Lunar Materials to Earth Orbit," AIAA–83-1344, June 1983.
[30] Taylor, L. A., and Carrier, W. D., "Oxygen Production on the Moon: An Overview and Evaluation," in *Resources of Near Earth Space*, eds. Lewis, J., Matthews, M. S., and Guerrieri, M. L., Tuscon University Press, pp. 69-108, 1993.
[31] Christiansen, E. L., et al., "Conceptual Design of a Lunar Oxygen Pilot Plant," EEI Report No. 88-182, Eagle Engineering, Inc., Houston, TX, July 1988.
[32] Allen, C. C., Weitz, C. M., and McKay, D. S., "Prospecting for Lunar Oxygen with Gamma Ray Spectrometry and Multispectral Imaging," in *Workshop on New Views of the Moon: Integrated Remotely Sensed, Geophysical, and Sample Datasets*, eds. Jolliff, B. L., and Ryder, G., LPI Contribution No. 958, Lunar and Planetary Institute, Houston, pp. 19-20, 1998.
[33] Watson, K., Murray, B. C., and Brown, H., "The Behavior of Volatiles on the Lunar Surface," *Journal of Geophysical Research*, 66, pp. 3033-3045, 1961.
[34] Arnold, J. R., "Ice in the Lunar Polar Regions," *Journal of Geophysical Research*, 84, pp. 5659-5668, 1979.
[35] Nozette, S., et al., "The Clementine Bistatic Radar Experiment," *Science*, 274, pp. 1495-1498, 1996.
[36] Feldman, W. C., et al., "Polar Hydrogen Deposits on the Moon," *Journal of Geophysical Research,* 105, pp. 4175-4195, February 25, 2000.
[37] "NASA Radar Finds Ice Deposits at Moon's North Pole," NASA Press Release, March 1, 2010, https://www.nasa.gov/home/hqnews/2010/mar/HQ_10-055_moon_ice.html.
[38] Spudis, P. D., et al., "Evidence for Water Ice on the Moon: Results for Anomalous Polar Craters from the LRO Mini-RF Imaging Radar," *Journal of Geophysical Research: Planets*, 118, pp. 1-14, 2013.
[39] Colaprete, A., et al., "Detection of Water in the LCROSS Ejecta Plume," *Science*, 330, pp. 463–468, 2010.
[40] Spudis, P. D., et al., "Initial Results for the North Pole of the Moon from Mini-SAR, Chandrayaan-1 Mission," *Geophysical Research Letters*, 37, L06204, March 31, 2010.
[41] http://www.mining.com/the-worlds-10-coldest-mines/.
[42] Amos, J., "'Coldest Place' Found on the Moon," http://news.bbc.co.uk/1/hi/sci/tech/8416749.stm, BBC, December 16, 2009.
[43] http://www.permanent.com/mining-the-moon-for-lunar-resources.html.
[44] Gertsch, L. S., and Gertsch. R. E., "Surface Mine Design and Planning for Lunar Regolith Production," STAIF-2003, AIP Conference Proc., Vol. 684, pp. 1108-1115, 2003.
[45] Podnieks, E. R., and Siekmeier, J. A., "Lunar Surface Mining Equipment Study," in Proc. 3rd International Conference on Engineering, Construction and Operations in Space III, eds. Sadeh, W. Z., et al., American Society of Civil Engineers, pp. 1104-1115, 1992.
[46] Podnieks, E. R., and Siekmeier, J. A., "Terrestrial Mining Technology Applied to Lunar Mining," in *Space Manufacturing 9: The High Frontier Accession, Development and Utilization*, Proc. of the Eleventh Space Studies Institute -Princeton Conference, ed. Faughnan, B., published by the American Institute of Aeronautics and Astronautics, pp. 301-308, September 1993.
[47] Gustafson, R. J., and Rice, E. E., "Lunar Polar Ice: Methods for Mining the New Resource for Exploration" AIAA-99-0850, January 1999.
[48] Ethridge, E., and Kaulker, W., "Microwave Extraction of Water from Lunar Regolith Simulant," STAIF-2007, AIP Conference Proc., Vol. 880, pp. 830-837, 2007.
[49] Colaprete, A., "Resource Prospector: Evaluating the ISRU Potential of the Lunar Poles," presentation to the Lunar Exploration Analysis Group (LEAG), November 2, 2016.
[50] Gertsch, L. S., Gustafson, R. J., and Gertsch. R. E., "Effect of Water Ice Content on Excavatability of Lunar Regolith," STAIF-2006, AIP Conference Proc., Vol. 813, pp. 1093-1100, February 2006.
[51] Gertsch, L. S., Rostami, J., and Gustafson, R. J., "Review of Lunar Regolith Properties for Design of Low Power Lunar Excavators," Paper No. 10.02, 6th International Conf on Case Histories in Geotechnical Engineering, August 2008.
[52] Koeing, D. R., "Experience Gained from the Space Nuclear Rocket Programs (Rover/NERVA)," Los Alamos National Laboratory, Report LA-10062-H, Los Alamos, NM, May 1986.
[53] Bulman, M. J., and Neill, T. M., "Simulated LOX-Augmented Nuclear Thermal Rocket (LANTR) Testing," AIAA–2000-3897, July 2000.

[54] https://en.wikipedia.org/wiki/RL10.
[55] Hodge, J., et al., "Space Transfer Vehicle – Lunar Transportation Ground Based LEO Rendezvous & Docking Study", NAS8-37856, Martin Marietta, August 1991.
[56] Ryan, S. W., and Borowski, S. K., "Integrated System Modeling for Nuclear Thermal Propulsion," AIAA–2014-3624, July 2014.
[57] http://www.history.com/topics/conestoga-wagon.
[58] Courtesy of the Landis Valley Village & Farm Museum, Pennsylvania Historical and Museum Commission.
[59] *2001: A Space Odyssey*, produced and directed by S. Kubrick, screenplay by S. Kubrick and A. C. Clarke, a Metro-Goldwyn-Mayer (MGM) film released 1968.
[60] Clarke, A. C., *2001: A Space Odyssey*, based on a screenplay by S. Kubrick an A. C. Clarke, a Signet Book, published by The New American Library, Inc., July 1968, p. 61.
[61] Sviatoslavsky, I. V., "Processing and Energy Costs for Mining Lunar Helium-3," in Workshop Proc. on Lunar Helium-3 and Fusion Power," NASA CP-10018, pp. 129-146, 1988.
[62] Williams, J.-P., et al., "The global surface temperature of the Moon as measured by the Diviner Lunar Radiometer Experiment," *Icarus*, 283, pp. 300-325, February 2017.
[63] Smitherman, D., and Woodcock, G., "Space Transportation Infrastructure Supported by Propellant Depots," AIAA–2011-7160, September 2011.